How Can Graph Theory Inform the Dual-stream Model of Speech Processing? A Resting-state Functional Magnetic Resonance Imaging Study of Stroke and Aphasia Symptomology

Haoze Zhu[1], Megan C. Fitzhugh[2], Lynsey M. Keator[3], Lisa Johnson[4], Chris Rorden[4], Leonardo Bonilha[5], Julius Fridriksson[4], and Corianne Rogalsky[1]

Abstract

■ The dual-stream model of speech processing describes a cortical network involved in speech processing. However, it is not yet known if the dual-stream model represents actual intrinsic functional brain networks. Furthermore, it is unclear how disruptions after a stroke to the functional connectivity of the dual-stream model's regions are related to speech production and comprehension impairments seen in aphasia. To address these questions, in the present study, we examined two independent resting-state fMRI data sets: (1) 28 neurotypical matched controls and (2) 28 chronic left-hemisphere stroke survivors collected at another site. We successfully identified an intrinsic functional network among the dual-stream model's regions in the control group using functional connectivity. We then used both standard functional connectivity analyses and graph theory approaches to determine how this connectivity may predict performance on clinical aphasia assessments. Our findings provide evidence that the dual-stream model of speech processing is an intrinsic network as measured via resting-state MRI and that functional connectivity of the hub nodes of the dual-stream network defined by graph theory methods, but not overall average network connectivity, is weaker in the stroke group than in the control participants. In addition, the functional connectivity of the hub nodes predicted linguistic impairments on clinical assessments. In particular, the relative strength of connectivity of the right hemisphere's homologues of the left dorsal stream hubs to the left dorsal hubs, versus to the right ventral stream hubs, is a particularly strong predictor of poststroke aphasia severity and symptomology. ■

INTRODUCTION

In the past two decades, the dual-stream model of speech processing[1] (Hickok & Poeppel, 2000, 2004, 2007) has, arguably, emerged as the prominent functional anatomical model of speech perception and production (Keator, Yourganov, Faria, Hillis, & Tippett, 2022; Rogalsky & Hickok, 2009; Spitsyna, Warren, Scott, Turkheimer, & Wise, 2006; Crinion & Price, 2005; Vandenberghe, Nobre, & Price, 2002; Humphries, Willard, Buchsbaum, & Hickok, 2001). During this same time, the connectivity of brain regions with similar response properties has emerged as a valuable predictor of behavioral performance and neurological disease (Keator et al., 2021; Zhang, Kucyi, et al., 2021; Battistella et al., 2020; Stone et al., 2020; Ferguson et al., 2019; Fitzhugh, Hemesath, Schaefer, Baxter, & Rogalsky, 2019; Walsh, Baxter, Smith, & Braden, 2019; Avants, 2018; Zhu et al., 2016). However, it remains unclear if the dual-stream model of speech processing represents an intrinsic, coherent brain network, and, if so, the nature of its organizational structure and how damage to one part of the network affects overall network function and speech performance remains unclear. Resting-state fMRI is a particularly promising, emerging tool to explore the dual-stream network as it relates to poststroke aphasia severity and specific impairments.

It is well established that low-frequency BOLD signal fluctuations at rest indicate coherent language-related neural activity (Battistella et al., 2020; Xu, Huang, Cui, & Yu, 2020; Zhao, Ralph, & Halai, 2018; Tie et al., 2014; Binder et al., 1999). For instance, a recent study by Battistella and colleagues (2020) identified several language-related networks with resting-state fMRI in young neurotypical adults, including dorsal articulatory-phonological and ventral semantic networks. Functional connectivity studies have also found significant functional connectivity across language-related areas in control participants, such as between sensorimotor areas and expressive and receptive language regions (Hampson, Peterson, Skudlarski, Gatenby, & Gore, 2002; Cordes et al., 2000). Thus, there is strong evidence that nodes of language networks are connected at rest; however, the architecture of these networks at rest have not been well mapped,

[1]Arizona State University, [2]University of California, San Diego, [3]University of Delaware, [4]University of South Carolina, [5]Emory University, Atlanta

Journal of Cognitive Neuroscience 37:3, pp. 737–766
https://doi.org/10.1162/jocn_a_02278

particularly in older adult control participants and stroke survivors.

Previous work has also begun to explore resting-state functional connectivity in individuals with stroke and aphasia, generally finding that functional connectivity differences are associated with treatment outcomes and behavioral measures of speech-processing abilities (e.g., Stockbridge et al., 2023; Xie et al., 2023; Chen et al., 2021; Klingbeil, Wawrzyniak, Stockert, & Saur, 2019; Siegel et al., 2016; Carter, Shulman, & Corbetta, 2012). A recent study conducted during the subacute phase of stroke revealed that participants who responded more to treatment exhibited significantly increased connectivity between the left fusiform gyrus and both ipsilateral and contralateral regions such as Broca's area and the superior temporal gyrus, compared with their lower responding counterparts. This finding suggests a potential restoration of proximal connectivity and compensatory reorganization in contralateral regions (Stockbridge et al., 2023). Another study observed that individuals with aphasia displayed lower local efficiency in nodes across the whole brain compared with the control group, and local efficiency was positively correlated with language performance (Chen et al., 2021). The authors' interpretations of their findings are informed by the dual-stream model of speech processing, but it remains unclear if the dual-stream model is in fact is a network at rest and, if so, how its connectivity is affected by stroke.

The functional connectivity studies described above typically employed anatomically defined ROIs as seeds to identify correlations with other ROIs or voxels that predicted speech processing abilities. In addition to these traditional functional connectivity methods to characterize networks in resting-state fMRI, graph-theoretical approaches may be a powerful method to better understand the network properties of the dual-stream model's regions because they can identify hub regions that play pivotal roles in the network organization, and they can characterize additional network-level properties, which are not reflected in simple functional connectivity correlation measures (He & Evans, 2010; He, Chen, & Evans, 2008). Typically, graph-theoretical analyses consist of a series of nodes and edges corresponding to the constituent units and interactions of a network (Liao, Vasilakos, & He, 2017; Barabási, 2012; Boccaletti, Latora, Moreno, Chavez, & Hwang, 2006). Unlike traditional functional connectivity that focuses on the relationship between a few regions, graph theory tends to describe the organization of the whole network or the local node cluster. After building a graph, hub regions can be defined as the average shortest path length (Achard, Salvador, Whitcher, Suckling, & Bullmore, 2006). The shortest path length is the number of edges comprising the shortest path between any pair of nodes; the average shortest path length is the mean of the $n-1$ minimum pathway between the index node and all other nodes in the networks (Achard et al., 2006).

A few studies related to language in adult control participants and children have applied the graph theory to depict the interactions between brain regions known to be involved in speech processing, with greater performance on various language measures being related not only just to increased functional connectivity but also to increased connectivity of hub regions, as defined by graph theory approaches (Xiao, Friederici, Margulies, & Brauer, 2016; Muller & Meyer, 2014). In the area of degenerative brain disease, hub regions have been shown to be more vulnerable (Achard et al., 2006; Bassett & Bullmore, 2006; Albert, Jeong, & Barabási, 2000), in that damage to or disruptions of hub regions are typically more correlated with more severe neurocognitive impairments than damage or disruption to nonhub regions of a network (Roger et al., 2019; Stam, De Haan, Daffertshofer, Jones, & Manshanden, 2009; He et al., 2008). However, to our knowledge, no previous studies have examined the functional network connectivity of the dual-stream model using graph theory, and only a few studies have investigated stroke-induced language impairments using a graph theory more broadly (Mazrooyisebdani, Nair, Garcia-Ramos, & Prabhakaran, 2018; Duncan & Small, 2016; Bohland, Kapse, & Kiran, 2014). These previous studies found that some network-level properties were different in individuals with aphasia compared with control groups and that these properties were correlated with aphasia severity or specific types of language impairments. However, the discussion of functional connectivity between the hubs was absent. By moving beyond the more typical functional connectivity analyses and using graph theory, we will be able to examine network organization and reorganization in stroke survivors in new ways that can potentially help us better understand poststroke compensation and language impairments.

In the present study, we not only extend the study of the dual-stream model to resting-state fMRI but also implement graph theory approaches in both stroke survivors and neurotypical control participants to characterize how the dual-stream network differs because of stroke and is related to language abilities poststroke. We have three hypotheses: (1) The neurotypical control participants will exhibit strong resting-state functional connectivity patterns across dual-stream nodes that have been defined by previous task-based findings; (2) the stroke survivors, in comparison to the control group, will exhibit functional connectivity and graph theory parameter differences; and (3) in stroke survivors, differences to the hub regions defined by the graph theory will predict impairments in our behavioral language measures.

METHODS

Participants

Stroke Group

Twenty-nine chronic left-hemisphere stroke survivors were recruited and tested at the University of South

Carolina as part of an ongoing study of the neurobiology of speech and language. Sample size was based on prior studies using similar outcome measures that yielded robust findings with about 30 or less participants in each group (Chen et al., 2021; Fitzhugh, Schaefer, Baxter, & Rogalsky, 2021; Fitzhugh et al., 2019; Khazaee, Ebrahimzadeh, & Babajani-Feremi, 2015; Braun et al., 2012; Liu et al., 2008). One of the stroke participants' data was removed from the present study's analyses because of substantial head motion during scanning. Remaining stroke survivors range in age from 35 to 78 years (M = 60.00, SD = 11.47). Inclusion criteria included chronic stroke (>6 months before testing), right-handed pre-stroke, native speakers of American English, 18+ years of age, and with no history of neurological disease, head trauma, or psychiatric disturbances before their stroke (self-report and supported by review of MRI scans by a clinical neurological radiologist). Aphasia classification was determined by the Western Aphasia Battery–Revised (WAB; Kertesz, 2007); each stroke participant's aphasia diagnosis is reported in Table 1. The lesion overlap map (Figure 1) and proportion of damaged ROIs (Table 4) characterize the distribution of lesion locations for the stroke group.

Table 1. Demographics of the Stroke Group

Participant	*Sex*	*Age*	*Months Post Stroke*	*Years of Education*	*Aphasia Diagnosis*	*Aphasia Quotient*
M1001	Female	74	83	17	Conduction	63.4
M1004	Male	60	14	12	Broca's	52.1
M1006	Male	71	233	16	Broca's	45.9
M1008	Female	70	13	13	Broca's	37.6
M1015	Male	55	80	16	Broca's	52.9
M1022	Female	56	200	18	None	99.6
M1027	Male	46	19	12	Broca's	23
M1029	Male	69	15	18	Anomic	77.2
M1031	Male	73	29	12	Broca's	57.8
M1040	Female	37	14	19	Broca's	65.5
M1044	Male	66	109	16	Broca's	53.7
M1045	Male	51	47	12	Conduction	86
M1046	Male	58	19	20	Anomic	82.3
M1048	Female	35	14	15	Anomic	90.6
M1050	Female	68	22	16	Broca's	27.7
M1052	Male	38	34	12	Transcortical motor	77.4
M1053	Male	60	25	12	Broca's	31.4
M1057	Male	50	16	18	Broca's	28.8
M1058	Female	64	20	12	Global	14.5
M1061	Male	55	12	12	None	99.4
M1064	Male	62	14	16	Broca's	57.9
M1065	Male	75	12	18	Anomic	85
M1066	Male	63	127	19	Anomic	71
M1068	Male	65	12	16	Wernicke's	34.4
M1071	Male	53	16	14	Conduction	65.2
M1075	Female	78	13	16	Conduction	65.6
M1076	Female	67	87	17	None	97.8
M1079	Female	61	23	16	Conduction	83.4

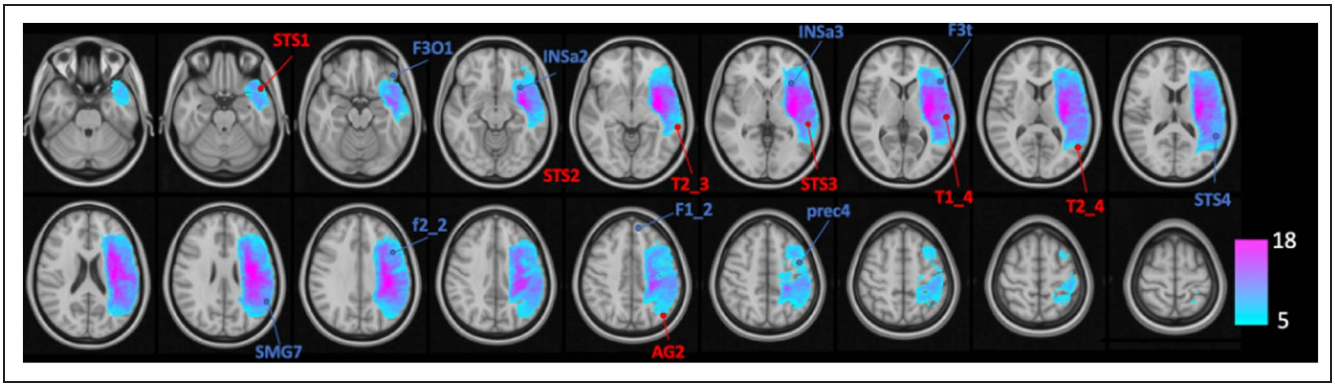

Figure 1. Lesion overlap map of the stroke group.

Control Group

Twenty-eight neurotypical adults ranging in age from 20 to 79 years (M = 58.79 years, SD = 18.72 years) who were also right-handed, native speakers of American English, 18+ years of age, have a minimum score of 27 on the Mini-Mental State Examination (Tombaugh & McIntyre, 1992), with no history of neurological disease, head trauma, or psychiatric disturbances were recruited from the greater Phoenix, Arizona, area. There were no significant differences between groups on age or sex, but the control group did have significantly more years of education than the stroke group, 15 versus 17 years, $t(54) = -2.42$, $p = .02$ (see Table 2).

This study was approved by Arizona State University institutional review board. All participants provided written informed consent.

Image Acquisition

Stroke Group

MRI data of the stroke group were acquired on a 3 T Siemens scanner equipped with a 12-channel radiofrequency head coil at Prisma Health Richland Hospita l (Columbia, South Carolina). A T2 structural image was collected with the following parameters: echo time = 57 msec, image size: (176 256 256), voxel size = 1 × 1 × 1 mm. Resting-state fMRI data were collected using EPI with the following parameters: one 11-min run, 427 total volumes, repetition time (TR) = 1650 msec, percent phase field of view (FOV) = 100, 2-mm slice thickness, 90 × 90 matrix size of 2.4-mm voxels.

Control Group

MRI data of the control group were acquired on a 3 T Phillips Ingenia MRI scanner equipped with a 32-channel radiofrequency head coil located at the Keller Center for Imaging Innovation at the Barrow Neurological Institute in Phoenix, Arizona. A T1 image was collected with the following parameters: FOV = 270 × 252, TR = 6.74 s, echo time = 3.10 msec, flip angle = 9, voxel size = 1 × 1 × 1 mm. Resting-state fMRI data were collected using EPI with the following parameters: one 10-min run, 197 total volumes, TR = 3000 msec, FOV = 217 × 217, matrix = 64 × 62, 3.39-mm slice thickness, in-plane resolution = 3.39 × 3.39 mm. Although the stroke and control groups' data were acquired from different scanners, there is evidence that interscanner variability effects on functional connectivity, such as we use here, is limited (Belleau et al., 2020; Marek et al., 2019; Noble et al., 2017).

Behavioral Data Methods

The language abilities of the stroke group were evaluated by the administration of the WAB (Kertesz, 2007). The WAB's aphasia quotient indicating overall aphasia severity, as well as the scores of the following subtests, were used in subsequent analyses: Spontaneous Speech, Auditory Verbal Comprehension, Repetition, Naming, and Word Finding.

Table 2. Comparison of Demographics of Stroke and Control Groups

	Stroke (n = 28)	*Control (n = 28)*	*Group Comparison Statistic*
Age: mean years (*SD*)	60.00 (11.47)	58.79 (18.72)	$t(54) = 0.29$, $p = .77$
Sex: male/female	18/10	14/14	$\chi^2(1) = 1.1667$, $p = .28$
Education: mean years (*SD*)	15.36 (2.60)	17.18 (3.01)	$t(54) = -2.42$, $p = .02$

Data Analysis

MRI Data Preprocessing

All resting-state fMRI data were preprocessed using Statistical Parametric Mapping 12 (https://www.fil.ion.ucl.ac.uk/spm). The first 10 time points of each run were discarded to ensure that the magnetization reached a steady state and the participants adapted to the environment. Slice timing was adjusted to compensate for the interleaved acquisition in the remaining 187 volumes for control and 427 volumes for stroke participants. Next, realignment was conducted to correct the head motion using the six standard head motion parameters. Then, the structural image (i.e., the T1-weighted image for the control group and the T2-weighted image for the stroke group) was reoriented to the mean functional image. Diffeomorphic anatomical registration through exponentiated Lie algebra normalization (Ashburner, 2007) was used to segment the structural image to white matter (WM), gray matter, and cerebral spinal fluid and normalize it to the Montreal Neurological Institute (MNI) template. Using the normal parameters of the structural image generated by diffeomorphic anatomical registration through exponentiated Lie algebra normalization, the functional images were spatially normalized to MNI space. Nuisance covariates including the WM signal, the cerebral spinal fluid signal, and head motion parameters were regressed out from the functional signal. To further ensure that our results are not driven by motion effects, we examined the relationship between motion and functional connectivity by computing correlations between the network-level functional connectivity and the mean motion measurement (from the six head motion parameters extracted during preprocessing; Van Dijk, Sabuncu, & Buckner, 2012), for each part of the dual-stream speech-processing network that we investigated. No significant correlations were found, and thus, no further action was taken regarding motion effects. We then applied band-pass filtering between 0.01 and 0.1 Hz and spatial smoothing with an 8-mm FWHM Gaussian kernel to facilitate group analyses. For the stroke group's fMRI data processing, we also added a cost function masking step (Andersen, Rapcsak, & Beeson, 2010; Brett, Leff, Rorden, & Ashburner, 2001) to avoid the risk that a stretched or altered perilesion tissue would impair normalization. The mask used in this step was generated from a manual demarcation of the chronic stroke lesion as seen on the T2-weighted images by researchers trained in neuroanatomy and lesion mapping procedures.

Identification of Nodes in the Dual-stream Network

There are several meta-analysis studies and reviews that identify left dominant regions that are involved in speech processing, including regions in the left frontal, temporal, and parietal lobes (Klingbeil et al., 2019; Mesulam et al., 2014; Margulies & Petrides, 2013; Price, 2012; Dronkers, 2011; Vigneau et al., 2006), which is in line with the dual stream model. To depict these comprehensive speech processing areas, we used 32 nodes from a previous task-based fMRI study in the left hemisphere, which used three contrasts including sentence production, listening, and reading, with corresponding word-list reference tasks (Labache et al., 2019). These regions are highly consistent with typical language areas found in other studies and reviews. Out of the Labache and colleagues coordinates, the coordinates within the precentral sulcus, superior frontal gyrus, inferior frontal sulcus, Broca's area, anterior insula, supramarginal gyrus, and posterior superior temporal sulcus were classified as dorsal; other coordinates in the superior temporal gyrus, middle temporal gyrus, superior temporal sulcus, and angular gyrus were classified as ventral, based on the location. All the nodes in the left hemisphere are listed in Table 3. Table 4 indicates the proportion of the participants in the stroke group who have lesions within the boundary of each node (i.e., a 6-mm radius sphere around the peak coordinates), as defined by the lesion demarcation procedure based on the T2 structural MRIs. To examine the influence of structural lesions within the functional connectivity nodes on subsequent analyses, we also identified stroke participants with lesions in more than 50% of the left hemisphere dual-stream nodes' centers of mass (i.e., lesions on the Labache et al., 2019, coordinates used to define the nodes). Four participants were identified using this threshold; the between-group comparisons and regression analyses within the stroke group described below were then conducted with and without these four participants.

Functional Connectivity

Functional connectivity was computed between nodes. The nodes were defined as 6-mm radius spheres around the peak coordinates reported in Labache and colleagues (2019). To better fit the dual-stream model's bilateral ventral streams, we also included the homologue of temporal and parietal nodes in the right hemisphere to study the activity in the right ventral (RV) stream. We then calculated the Pearson correlation coefficients between each pair of nodes; correlation coefficients were then Fisher transformed. To explore possible functional reorganization in the right hemisphere in response to the left dorsal (LD) stream damage, we also included potential right dorsal (RD) stream nodes using the homologue coordinates of the left hemisphere's dorsal stream's nodes. All the functional connectivity analyses were performed using in-house scripts executed in MATLAB. The average functional connectivity matrices of the control and stroke groups are shown in Figure 2.

Defining the Dual-stream Speech Processing Network in Control Participants

To confirm that the neural correlates of the dual-stream model do in fact form a significant network in our neurotypical control participants, we computed the following

Table 3. Left-hemisphere Nodes

Region	*MNI Coordinates*	*Abbreviation (in Labache et al., 2019)*	*Category*
Precentral sulcus – 4	−42.2, 0.7, 49.9	prec4	Dorsal
Superior frontal gyrus – 2	−11.9, 46.5, 41.4	F1_2	Dorsal
Inferior frontal sulcus – 2	−43.1, 14.8, 29.4	f2_2	Dorsal
Inferior frontal pars triangularis gyrus – 1	−49.4, 25.6, 4.7	F3t	Dorsal
Inferior frontal pars opercularis gyrus – 1	−42.2, 30.5, –16.9	F3O1	Dorsal
Anterior insula gyrus – 2	−33.8, 16.8, –12.7	INSa2	Dorsal
Anterior insula gyrus – 3	−33.7, 23.7, 0.6	INSa3	Dorsal
Superior temporal sulcus – 4	−56.5, −48.4, 13.4	STS4	Dorsal
Supramarginal gyrus – 7	−55.2, −51.7, 25.5	SMG7	Dorsal
Superior temporal gyrus – 4	−58.7, −23.3, 3.7	T1_4	Ventral
Middle temporal gyrus – 3	−61.0, −35.0, −4.8	T2_3	Ventral
Middle temporal gyrus – 4	−53.1, −59.4, 7.0	T2_4	Ventral
Superior temporal sulcus – 1	−49.7, 14.0, −21.5	STS1	Ventral
Superior temporal sulcus – 2	−54.9, −7.2, −12.8	STS2	Ventral
Superior temporal sulcus – 3	−54.7, −33.0, −1.7	STS3	Ventral
Angular gyrus – 2	−37.5, −70.4, 39.5	AG2	Ventral
Precentral sulcus – 3	−18.2, −8.7, 69.3	pre3	Others
Anterior Insula gyrus – 1	−20.3, 5.0, −19.3	INSa1	Others
Inferior Temporal gyrus – 4	−50.0, −60.6, −7.6	T3_4	Others
Inferior occipital gyrus – 1	−48.4, −69.0, −4.3	O3_1	Others
Fusiform gyrus – 4	−43.1, −49.8, −17.4	FUS4	Others
Parahippocampal gyrus – 1	−15.7, −4.0, −18.4	pHIPP1	Others
Hippocampus gyrus – 2	−24.9, −32.5, −2.7	HIPP2	Others
Superior motor area gyrus – 2	−10.6, 18.2, 63.1	SMA2	Others
Superior motor area gyrus – 3	−7.2, 7.6, 65.6	SMA3	Others
Paracentral lobule gyrus – 4	−6.4, −29.2, 75.9	pCENT4	Others
Posterior cingulum gyrus – 3	−5.1, −42.9, 10	CINGp3	Others
Precuneus gyrus – 6	−7.4, −61.3, 64.1	PRECU6	Others
Amygdala – 1	−21.9, −0.4, −11.5	AMYG	Others
Thalamus – 4	−3.2, −14.4, 8.4	THA4	Others
Putamen – 2	−23.3, 6.3, 0.8	PUT2	Others
Putamen – 3	−28.0, −6.3, 1.8	PUT3	Others

paired-samples *t* tests within the control group: (1) comparison of the average functional connectivity within the entire, bilateral dual-stream network, as well as the average connectivity in just the left-hemisphere nodes of the dual-stream network (i.e., between and within the LD and left ventral [LV] streams), with that of within the well-defined default mode and visual networks, and (2) comparison of the average functional connectivity between each stream of the dual-stream network (i.e., bilateral ventral and LD) to the average functional connectivity between the dual-stream nodes and those of the default mode network and visual network. The coordinates of the default mode network nodes (Table 5) used have been well defined by numerous previous resting-state and task-related fMRI

Table 4. Proportion of the Stroke Group Participants with at Least One Damaged Voxel in Each ROI

ROI Name	*Abbreviation*	*Proportion of Stroke Group with Damaged Voxels in the ROIs*
Precentral sulcus – 4	prec4	17.9%
Superior frontal gyrus – 2	F1_2	0%
Inferior frontal sulcus – 2	f2_2	28.6%
Inferior frontal pars triangularis gyrus – 1	F3t	35.7%
Inferior frontal pars opercularis gyrus – 1	F3O1	21.4%
Anterior insula gyrus – 2	INSa2	32.1%
Anterior insula gyrus – 3	INSa3	32.1%
Superior temporal sulcus – 4	STS4	39.3%
Supramarginal gyrus – 7	SMG7	39.3%
Superior temporal gyrus – 4	T1_4	39.3%
Middle temporal gyrus – 3	T2_3	25%
Middle temporal gyrus – 4	T2_4	21.4%
Superior temporal sulcus – 1	STS1	28.6%
Superior temporal sulcus – 2	STS2	35.7%
Superior temporal sulcus – 3	STS3	35.7%
Angular gyrus – 2	AG2	14.3%

studies (Zhu et al., 2016; Gao & Lin, 2012; Vincent, Kahn, Snyder, Raichle, & Buckner, 2008). The visual network coordinates (Table 5) were taken from a previous task-based fMRI study (Gao & Lin, 2012), which aligns well with numerous other works identifying this network (Tedeschi et al., 2016; Lee, Smyser, & Shimony, 2013; Schöpf et al., 2010; Van Den Heuvel & Pol, 2010). False discovery rate (FDR) correction was used to control the false positives at $p < .05$. All the statistical analyses including paired t tests, two-sample t tests, regression models, and multiple comparison corrections were coded in R (https://www.r-project.org/).

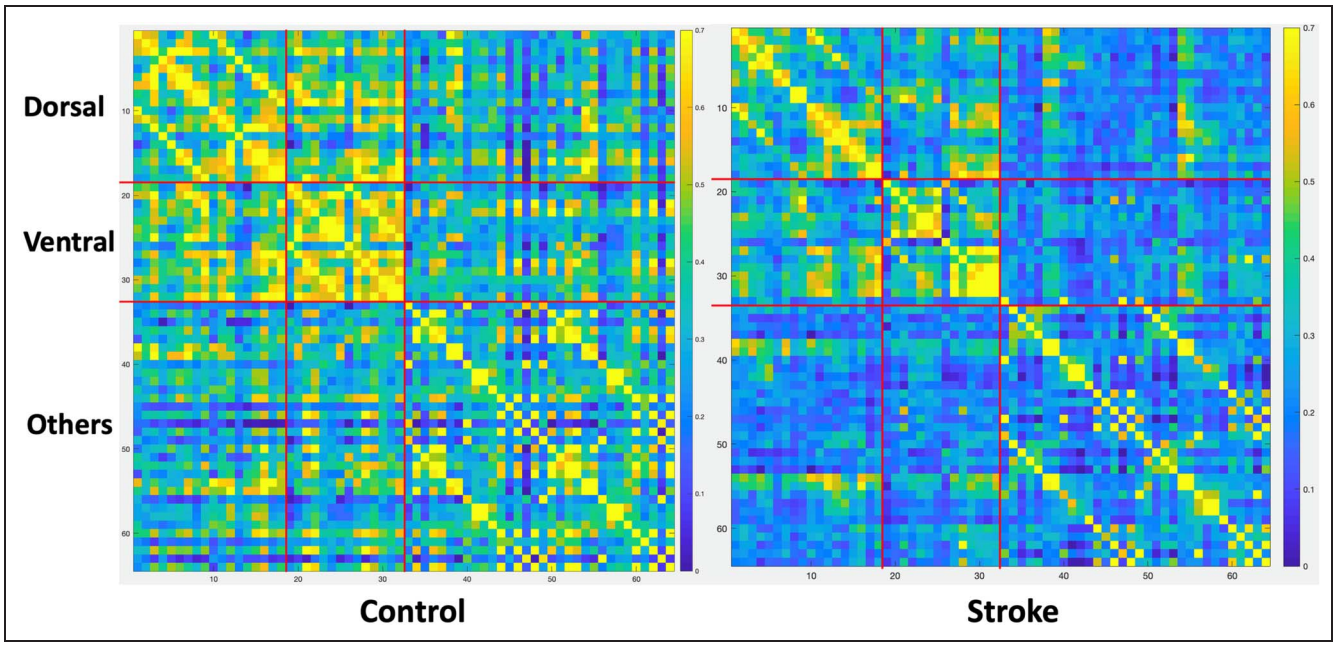

Figure 2. Stroke group network comparisons. Comparison of the functional connectivity within the dual-stream network, within only the left hemisphere of the dual-stream network (i.e., between and within the LD and ventral stream), the default mode network, and the visual network. An asterisk indicates statistical significance at $p < .05$, FDR corrected.

Table 5. Default Mode Network and Visual Network Nodes Examined for Comparison Purposes

Region	*MNI Coordinates*	*Category*
Left hippocampus formation	−21, −15, −14	Default mode
Right hippocampus formation	24, −19, −21	Default mode
Medial prefrontal cortex	0, 51, −7	Default mode
Posterior cingulate cortex	1, −55, 17	Default mode
Left posterior inferior parietal lobule	−47, −71, 29	Default mode
Right posterior inferior parietal lobule	50, −64, 27	Default mode
Left calcarine	−8, −72, 4	Visual
Right calcarine	16, −67, 5	Visual
Left cuneus	−5, −96, 12	Visual
Right cuneus	18, −96, 12	Visual
Left lateral occipital	−23, −89, 12	Visual
Right lateral occipital	37, −85, 13	Visual

Functional Connectivity of the Dual-stream Language Network in the Stroke Group

For the stroke group (in the same fashion as for the control group, described above), we computed the overall connectivity of the dual stream model network, as well as the left-hemisphere streams only and each stream separately, and compared them to that of the visual and default mode networks using paired-samples t tests with FDR correction to control false positives at $p < .05$.

Functional Connectivity Comparisons between Control and Stroke Groups

To compare the functional connectivity of the dual-stream nodes of the stroke group to those of the control group, we computed independent-samples t tests of the average functional connectivities between the stroke and control groups for the following groups of nodes: within left ventral, within LD, between LV and LD, between RD and RV, within RD, within RV, between left and RV, between LD and RD, and between LV, LD and RV. An FDR correction was used to control the false positives at $p < .05$.

Graph Theory Analysis

Using the functional connectivity correlations described above as the edges between the nodes, we used graph theory methods to extract the average shortest path lengths for each node to identify hub regions. The parameters for the graph construction are summarized in Table 6 (Achard et al., 2006; Humphries, Gurney, & Prescott, 2006). To obtain the average shortest path length, first, a

Table 6. The Measurements and Their Meaning in the Brain Functional Network (Liu et al., 2008; Achard et al., 2006)

Character	*Meaning*
N	The number of nodes
C_i	The cluster coefficient of a node
L_i	The shortest path length of a node. $L_i = \frac{1}{N-1}\sum_{i\neq j}\min\{L_{ij}\}$, in which min $\{L_{ij}\}$ is the shortest absolute path length between ith and jth nodes, and N is the number of nodes.
C_{net}	The cluster coefficient of network. It is the mean of C_i of all nodes.
L_{net}	The shortest path length of the network. It is the average shortest path length of all nodes
γ	$\gamma = C_{\text{net}}/C_{\text{ran}}$ The ratio of the clustering coefficients between real and random network
λ	$\lambda = L_{\text{net}}/L_{\text{ran}}$ The ratio of the path length between real and random network
σ	$\sigma = \gamma/\lambda$ Measurement of the small-wordness of a network
K	Mean degree
T	T = N * (n − 1)/2, maximum number of possible edges

binary undirected graph at varying thresholds of the functional connectivity was constructed, to identify an appropriate threshold for the subsequent analyses using small-world properties. In order for a graph to be classified as a small-world network, it must satisfy three requirements: (1) the ratio of cluster coefficient $\gamma = C_{net}/C_{ran} > 1$, (2) the ratio of path length $\lambda = L_{net}/L_{ran} \sim 1$, and (3) the "small worldness" ratio $\sigma > 1$ (Achard et al., 2006; Humphries et al., 2006; Montoya & Solé, 2002; Watts & Strogatz, 1998). To compute C_{ran} and L_{ran}, we applied randomized manipulation by a Markov-chain algorithm (Liu et al., 2008; Maslov & Sneppen, 2002) 100 times for each potential threshold and obtained C_{ran} and L_{ran} from the mean of 100 random networks. Then, we found an optimized threshold to attain a best balance between γ, λ, and σ ($\gamma > 1$, $\lambda \sim 1$, and $\sigma > 1$), using a search of the proportion of possible connections that actually exist between all the nodes. To ensure that the network is not too sparse and thus causing the small-world properties to be inestimable (Achard et al., 2006), the search began at K*N/T = 13.2% (see Table 6 for variables). The current study has 64 nodes for the graph theory analysis. The minimal edge number should be K * N, thus, in this case, equal to 266. Then, the maximum possible of edges (T) of a 64 × 64 matrix is 2016. Finally, K * N/T = 266/2016 is the minimum percentage (i.e., the beginning of the search). The end of the search is 20%, which was the maximum threshold to account for the known sparsity of a small-world organization (Roger et al., 2019; Achard & Bullmore, 2007).

We then identified "hub" nodes based on the mean shortest path lengths computed. Again, the mean shortest path length formula of a node is: $L_i = \frac{1}{N-1}\sum_{i \neq j} \min\{L_{ij}\}$. To be identified as a hub of the dual-stream network, a node must satisfy two criteria: (1) be one of the two nodes with the smallest values in the LD, right dorsal, left ventral, or RV streams, and (2) be a node with functional connectivity to at least half of the other nodes either directly or mediated by one or more nodes that passes the threshold defined above. Then, to continue our exploration of a possible right dorsal stream involvement in aphasia, we labeled the right homologues of the hubs in the LD stream as right dorsal hubs. The hub nodes defined above in the control group were used to calculate the functional connectivity between hub nodes in the stroke group. Independent-samples *t* tests then were used to detect differences between the control and stroke groups for functional connectivities within and between the streams' hub nodes. Once again, the significant results were FDR corrected to $p < .05$.

Regression Analysis of Hub Node Functional Connectivity to Predict Stroke Group Performance

The functional connectivities within each stream were used as predictors in multiple regression models (*lm* command in R) to predict each stroke survivor's performance on each WAB behavioral measure. The selection of the predictors included to predict each WAB measure was based on previous lesion-symptom mapping and task-based fMRI work (Kertesz, 2022; Fridriksson et al., 2018; Thye & Mirman, 2018; Baldo, Arévalo, Patterson, & Dronkers, 2013; Kümmerer et al., 2013; Shulman et al., 1997) and is summarized in Table 7. Lesion size, age, sex, and years of education were also included in each model as covariates. We applied a reduction of predictor variables using Akaike-information-criterion-based elimination in R (step order) to remove the predictors or covariates that contribute little to each model—a standard procedure to remove predictors that are not related to the response variable that could lead to an inflated prediction error (Chambers & Hastie, 1992). To identify potential collinearity between the hub functional connectivity predictors, we (1) implemented a multicollinearity test such that any pairs of predictors with a $|r| > 0.7$ (Dormann, Elith, Bacher, et al., 2013) would be considered as too highly correlated and one of the predictors should be removed to not inflate results, and (2) computed the variance inflation factor (VIF) for each predictor in each model; VIF > 5 would lead to the exclusion of that predictor in that model (Shrestha, 2020).

RESULTS

Functional Connectivity of the Dual-stream Model

Control Group

The paired-samples *t* tests computed within the control group to compare the mean functional connectivity within the dual-stream network with that of the other reference

Table 7. The Functional Connectivity Predictors for WAB-R

	L Dorsal	*R Dorsal*	*L Ventral*	*R Ventral*	*L Dorsal–Ventral*	*R Dorsal–Ventral*	*L & R Dorsal*	*L & R Ventral*
Spont. Speech	✓	✓			✓	✓	✓	
Auditory Verbal Comprehension			✓	✓	✓	✓		✓
Repetition	✓	✓	✓	✓	✓	✓	✓	✓
Naming and Word Finding	✓	✓	✓	✓	✓	✓	✓	✓
Aphasia Quotient	✓	✓	✓	✓	✓	✓	✓	✓

L = left; R = right; L & R Dorsal = between left and right dorsal; L & R Ventral = between left and right ventral.

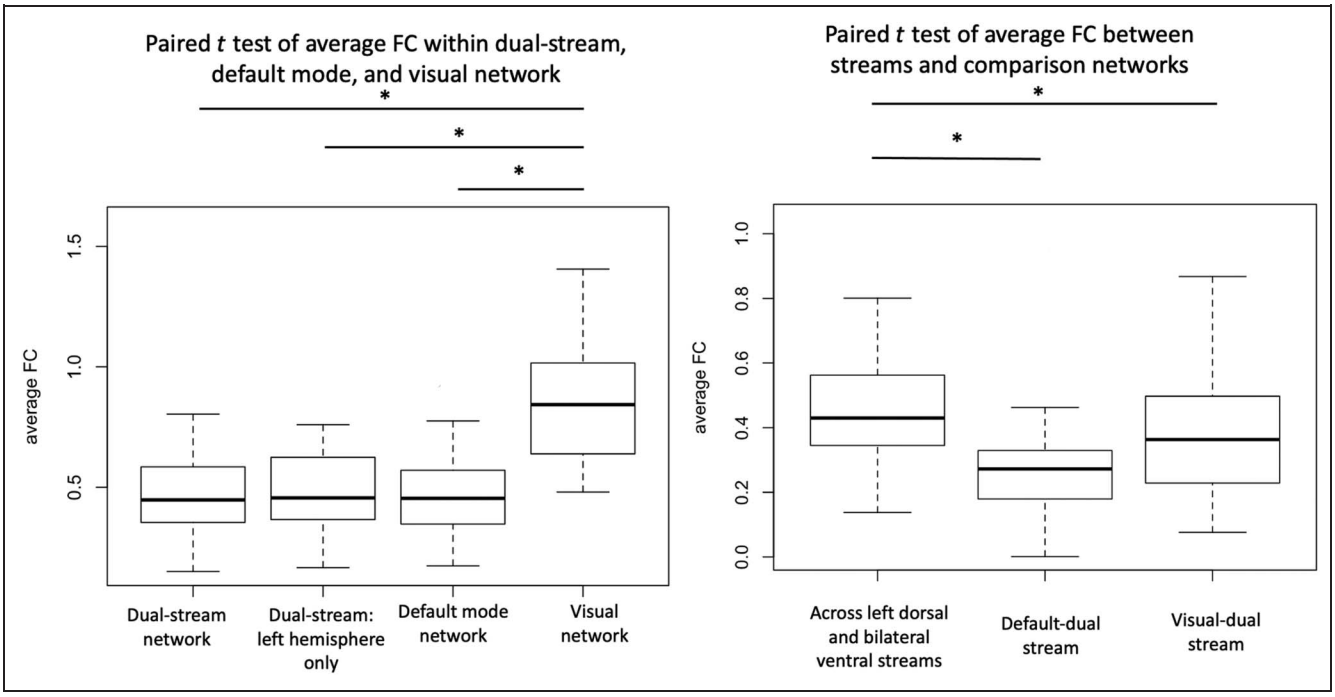

Figure 3. Mean functional connectivity of all nodes within different portions of the dual-stream network for the control and stroke groups. There is no significant result after the FDR correction at $p < .05$. The error bar indicates 1 *SD*.

networks yielded the following results: The functional connectivity of the visual network was significantly higher than that of the dual-stream network, $t(27) = 7.84$, FDR $p < .01$; the default mode network, $t(27) = 5.97$, FDR $p < .01$; and the left hemisphere-only dual-stream network, $t(27) = 7.65$, FDR $p < .01$ (Figure 3). There were no significant differences between the functional connectivity of the dual-stream and default mode networks, or between the dual stream and just the left hemisphere dual stream. The functional connectivity between LD and bilateral ventral streams was significantly higher than the connectivity between dual-stream regions and default mode network, $t(27) = 6.09$, FDR $p < .01$; the functional connectivity between LD and bilateral ventral streams also was significantly higher than the connectivity between dual-stream regions and visual network, $t(27) = 3.98$, FDR $p < .01$.

Stroke Group

Similar to the control group, the stroke group exhibited greater functional connectivity within the visual network than in the dual-stream network, $t(27) = 6.00$, FDR $p < .01$; the default mode network, $t(27) = 4.61$, FDR $p < .01$; or the left hemisphere-only dual-stream network, $t(27) = 6.16$, FDR $p < .01$ (Figure 4). No significant results were found between the dual-stream network, default mode network, and the left hemisphere-only dual-stream network.

Functional Connectivity Differences across Groups in Typical Dual-stream Regions

There were no significant differences between the stroke and control groups regarding the average functional connectivity in the dual-stream speech network as a whole or in any of the streams (Figure 5). The comparisons excluding the four stroke group participants with more than 50% lesioned left-hemisphere nodes (Figure A1) also

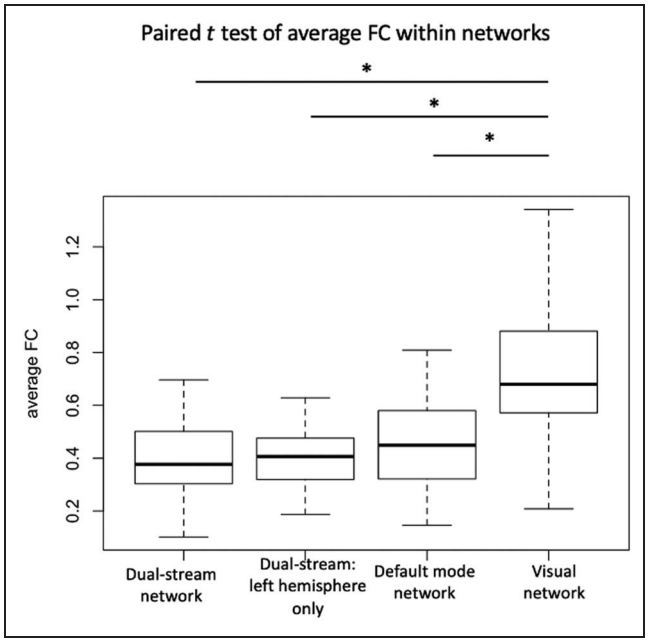

Figure 4. Average functional connectivity (z value after Fisher transformation) matrix with all the nodes (Labache et al., 2019) for the control group (left) and stroke group (right). Dorsal stream nodes involved the regions of precentral sulcus, superior frontal gyrus, inferior frontal sulcus, pars triangularis gyrus, pars opercularis, anterior insula, superior temporal sulcus, and supramarginal gyrus. Ventral stream nodes involved superior temporal gyrus, superior temporal sulcus, and angular gyrus. Table 3 indicates all the node locations.

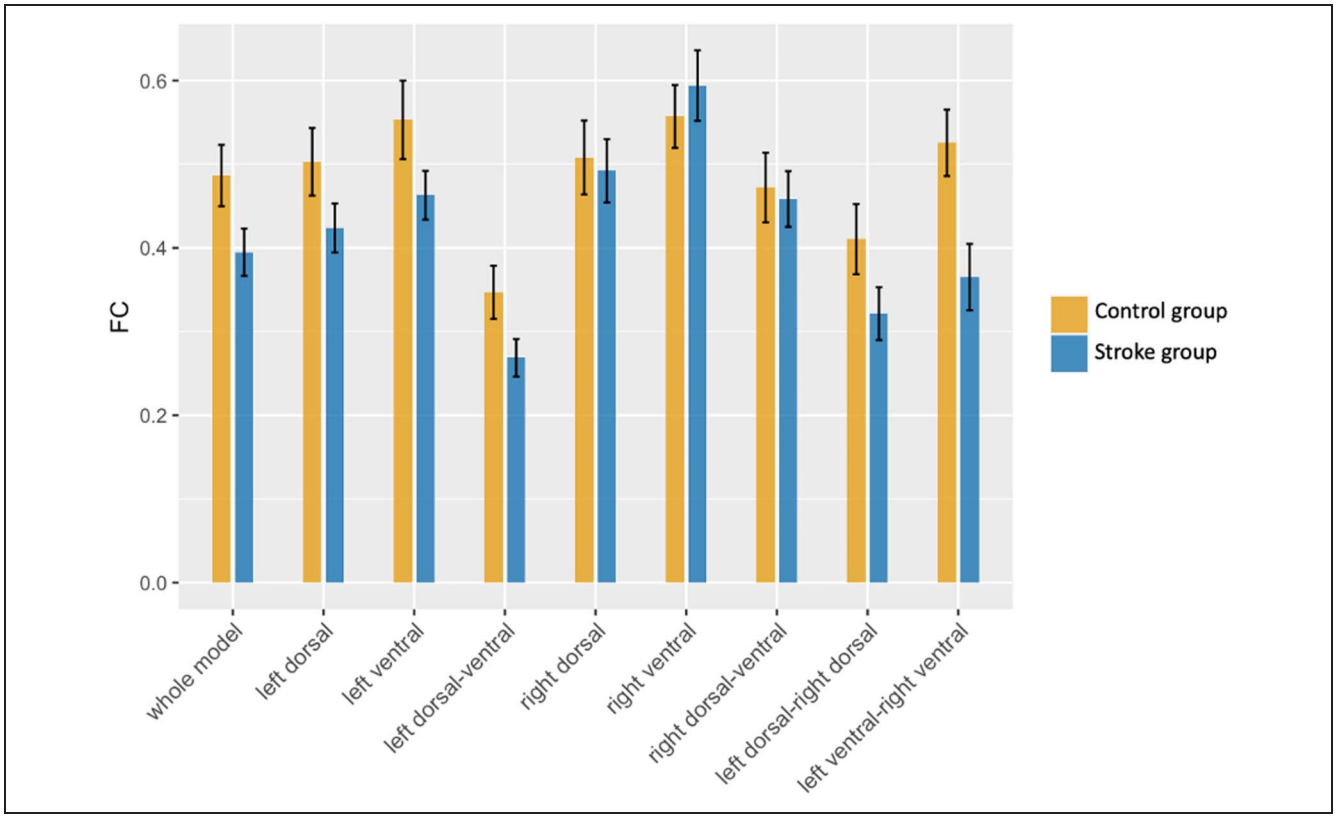

Figure 5. Control group network comparisons. Left: comparison of the functional connectivity within the dual-stream network, within the left hemisphere (between and within the LD and ventral stream), the default mode network, and the visual network. Right: comparison of the functional connectivity within the right dorsal and bilateral ventral streams. The asterisk indicates statistical significance at $p < .05$, FDR corrected.

yielded no significant differences between the stroke and control groups.

Construction of Graph with Small World Network Assumption

To construct a graph that satisfies the small world network assumption, we need $\gamma > 1$, $\lambda \sim 1$, and $\sigma > 1$ (Achard et al., 2006). Figure 6 indicates the trend of λ, γ, and σ as the proportion of connections is increased. The λ is closest to 1 at proportion 0.132, and the highest value of γ and σ also occur at threshold 0.132. Therefore, the best proportion of connections in our control group data is 0.132. At this threshold, λ is equal to 1.02, γ is equal to 1.06, and σ is equal to 1.04.

Hubs of the Dual-stream Network

Eight nodes of the dual-stream network were identified as hubs (defined by the top two ranked shortest path

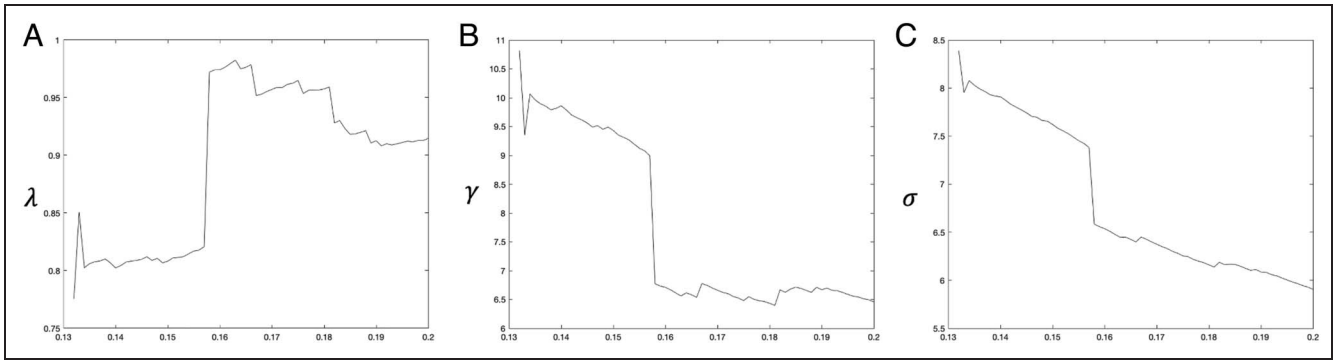

Figure 6. Small-world properties of the brain network as a function of proportion of connections. (A) Approaches 1 most at threshold 0.132; (B) has the highest value at threshold 0.132; (C) has the highest value at threshold 0.132.

Table 8. Properties of the Top-ranked Lower Average Path Length Nodes in Bilateral Dorsal and Ventral Streams

Category	*Region*	*Abbreviation*	*Path Length*	*Degree*	*Connected Nodes*
LD	**Left superior temporal sulcus**	**STS4**	**1.83**	**14**	**47**
	Left triangularis	**F3t**	**1.85**	**14**	**47**
	Left precentral	Prec4	1.87	14	47
	Left frontal	F3O1	2.02	10	47
Left ventral	**Left middle temporal gyrus**	**T2_4**	**1.79**	**18**	**47**
	Left superior temporal gyrus	**T1_4**	**2**	**16**	**47**
	Left temporal	STS3	2	12	47
Right dorsal	***Right superior temporal sulcus***	***STS4***	***2.02***	***11***	***47***
	Right precentral	Prec4	1.70	20	47
	Right triangularis	**F3t**	**1.87**	**14**	**47**
	Right frontal	f2_2	2	9	47
RV	**Right superior temporal sulcus**	**STS3**	**1.74**	**19**	**47**
	Right middle temporal gyrus	**T2_3**	**1.81**	**18**	**47**
	Right temporal	T1_4	1.98	14	47
	Right temporal	T2_4	2	16	47
	Right temporal	STS4	2.02	11	47
Others	Left cingulum	CINGp3	1	1	1
	Right cingulum	CINGp3	1	1	1

Bold indicates the hub nodes, and the *italics* indicate the right-hemisphere homologues of the LD hubs. Note that if we were to find the lowest average path length nodes as the hub in the right dorsal stream directly, the nodes identified remain the same.

length nodes in the LD, left ventral, and RV streams; right dorsal hubs are the homologue of the LD hubs). The hubs identified were the following nodes: left superior temporal sulcus and left pars triangularis in the LD stream, their homologues in the right dorsal stream, the middle portion of the left superior temporal gyrus and posterior portion of the left middle temporal gyrus in the left ventral stream, and the middle portion of the right middle temporal gyrus and the middle portion of the right superior temporal sulcus in the RV stream (Table 8 and Figure 7).

Functional Connectivity between Hubs in the Control and Stroke Groups

Independent *t* tests examining group functional connectivity differences of hub regions resulted in the following significant results (Figure 8): The functional connectivity

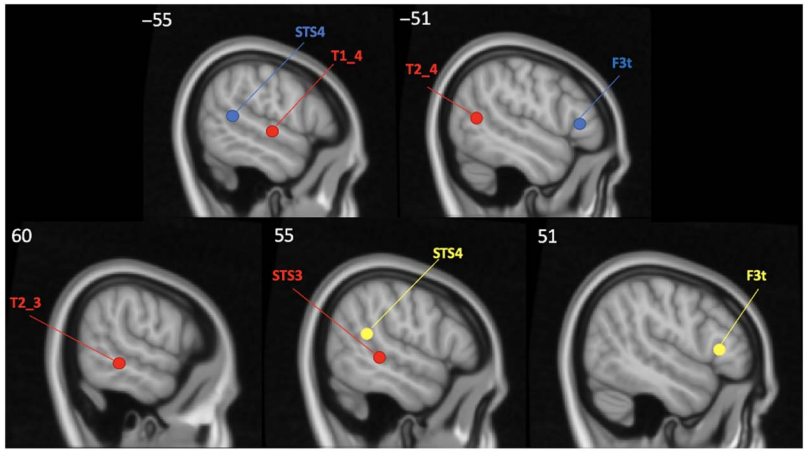

Figure 7. The hub nodes of the dual-stream language network identified in the control group. Red indicates the ventral stream, blue indicates the LD stream, and yellow indicates the right dorsal stream, which is the homologue of the LD stream. The top row indicates the hub nodes identified in the left hemisphere, and the bottom row indicates nodes identified in the right hemisphere. The caption of the nodes can be found in Table 3.

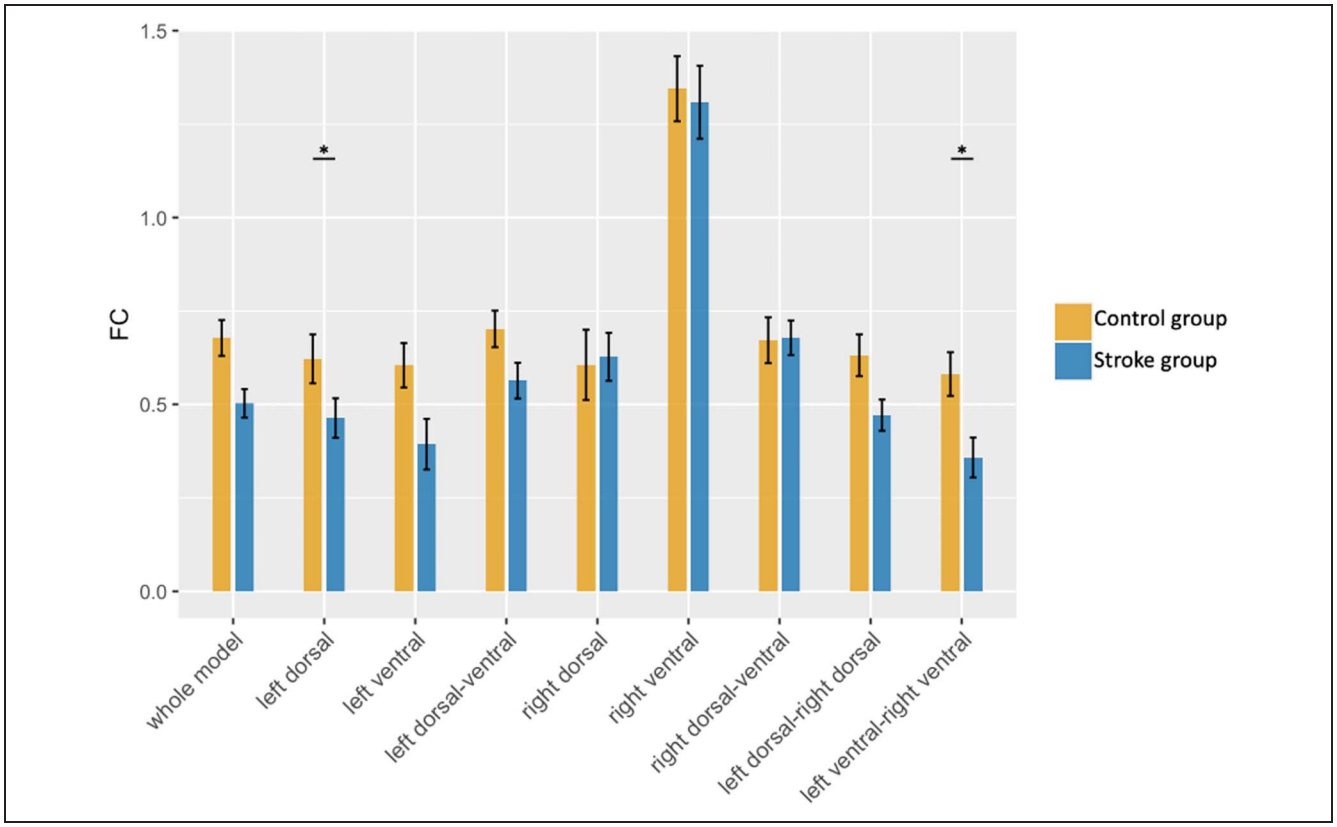

Figure 8. The between-group comparisons of functional connectivity of hubs across the control and stroke groups. The asterisk indicates a significant difference, $p < .05$, after FDR correction. The error bar indicates 1 *SD*.

within the LD stream of the control group was significantly higher than that of the stroke group, $t(54) = 2.84$, FDR $p = .03$, and the functional connectivity between the left ventral and RV streams of the control group was significantly higher than that of the stroke group, $t(54) = 2.30$, FDR $p = .03$. The between-group hub comparisons excluding the four stroke participants with more than 50% lesioned left-hemisphere nodes yielded no significant differences, although the values follow similar trends as in the whole data set, and three *t* tests approach significance after FDR correction: whole model, $t(50) = 2.34$, FDR $p = .087$; LV, $t(50) = 2.25$ FDR $p = .087$; and LV to RV, $t(50) = 2.45$, FDR $p = .087$ (Figure A2).

Regression Model to Predict WAB Performance with Hub Functional Connectivity

Our tests of multicollinearity indicate that multicollinearity does not need to be addressed further in the regression models: (1) No pair of predictors have a correlation of $|r| > 0.7$, and (2) no VIF > 5 was found (Table 9). Table 10 lists all of the results from the regression models predicting each WAB measure from the functional connectivities of the dual-stream network's hubs in the stroke group. Significant results were as follows: Spontaneous Speech's significant predictors were LD ($\beta = -15.44$, $t = -3.51$, $p < .01$) and right dorsal–ventral (RDV, $\beta = -7.21$, $t = -2.21$, $p = .05$) functional connectivity, as well

Table 9. The VIF of the Regression Model Using Hub Functional Connectivity Predictors

	L Dorsal	*R Dorsal*	*L Ventral*	*R Ventral*	*L Dorsal–Ventral*	*R Dorsal–Ventral*	*L & R Dorsal*	*L & R Ventral*
Spont. Speech	3.06	2.12	n/a	n/a	2.53	1.53	2.73	n/a
Auditory Verbal Comprehension	n/a	n/a	2.53	1.92	2.66	1.74	n/a	1.77
Repetition	3.46	2.47	3.15	2.03	2.66	2.16	3.81	2.37
Naming and Word Finding	3.46	2.47	3.15	2.03	2.66	2.16	3.81	2.37
Aphasia Quotient	3.46	2.47	3.15	2.03	2.66	2.16	3.81	2.37

Table 10. The Regression Model Using the Hub Functional Connectivity Predictors

	LD	*RD*	*RV*	*LDV*	*RDV*	*L&RD*	*F Test*
Spontaneous Speech	**β = −15.44** **t = −3.51** **p < .01**	–		β = 8.92 t = 1.96 p = .06	**β = −7.21** **t = −2.11** **p = .05**	β = 10.20 t = 2.06 p = .05	**$F(7, 20) = 4.66$, $p < .01$**
Auditory Verbal Comprehension			β = 0.99 t = 1.42 p = .17	–	**β = −3.17** **t = −2.13** **p = .04**		**$F(3, 24) = 4.68$, $p = .01$**
Repetition	**β = −4.92** **t = −2.92** **p = .01**	β = −2.19 t = −1.55 p = .14	**β = 2.11** **t = 2.44** **p = .03**	–	**β = −5.37** **t = −2.84** **p = .01**	–	**$F(9, 18) = 5.49$, $p < .01$**
Naming and Word Finding	**β = −5.38** **t = −3.08** **p < .01**	–	**β = 2.80** **t = 3.44** **p < .01**	–	**β = −6.88** **t = −3.75** **p < .01**	**β = 5.38** **t = 2.11** **p = .05**	**$F(7, 20) = 7.27$, $p < .01$**
Aphasia Quotient	**β = −56.83** **t = −3.13** **p < .01**	β = −14.91 t = −1.25 p = .23	β = 14.02 t = 1.94 p = .07	β = 25.99 t = 1.46 p = .16	**β = −41.74** **t = −2.67** **p = .02**	**β = 58.76** **t = 2.93** **p = .01**	**$F(9, 18) = 6.57$, $p < .01$**

The first column is the dependent variable from the Western Aphasia Battery, the following columns are the functional connectivity independent variables, and the last column is the *F* test of the regression model. Dependent variables: SS = spontaneous speech; AVC = Auditory Verbal Comprehension; RP = repetition; NWF = Naming and Word Finding; AQ = aphasia quotient. Independent variables: LD = left dorsal; RD = right dorsal; RV = right ventral; LDV = left dorsal-ventral; RDV = right dorsal-ventral; L&RV = between the left and right dorsal. Significant findings are in **bold**. The gray color indicates the predictor is not included in the initial model. The dash indicates the predictors are removed by Akaike-Information-Criterion-based elimination. Left ventral and between left and RV predictors were eliminated in every model, so they are excluded here.

as age ($\beta = -0.19$, $t = -2.64$, $p = .02$), education ($\beta = 0.78$, $t = 2.36$, $p = .03$), and lesion size ($\beta = -1.0e{-}04$, $t = -2.28$, $p = .03$). RDV functional connectivity ($\beta = -3.17$, $t = -2.13$, $p = .04$) and lesion ($\beta = -4.0e{-}05$, $t = -2.54$, $p = .02$) were the only significant predictors of the Auditory Verbal Comprehension score. Repetition scores were significantly predicted by LD ($\beta = -4.92$, $t = -2.92$, $p < .01$), bilateral dorsal (between the left and right dorsal [L&RD], $\beta = 6.55$, $t = 2.58$, $p = .02$), RV ($\beta = 2.11$, $t = 2.44$, $p = .03$), and RDV ($\beta = -5.37$, $t = -2.84$, $p = .01$) functional connectivity, as well as education ($\beta = 0.34$, $t = 2.20$, $p = .04$). Naming and Word Finding scores were significantly predicted by LD ($\beta = -5.38$, $t = -3.08$, $p < .01$), L&RD ($\beta = 5.38$, $t = 2.11$, $p = .05$), RV ($\beta = 2.80$, $t = 3.45$, $p < .01$), and RDV ($\beta = -6.88$, $t = -3.75$, $p < .01$) functional connectivity, as well as education ($\beta = 0.37$, $t = 2.34$, $p = .03$). Aphasia Quotient yielded the following significant predictors: LD ($\beta = -56.83$, $t = -3.13$, $p < .01$), L&RD ($\beta = 58.76$, $t = 2.93$, $p < .01$) and RDV ($\beta = -41.74$, $t = -2.67$, $p = .02$) functional connectivity, as well as education ($\beta = 3.76$, $t = 2.88$, $p < .01$). The regression models excluding the four stroke participants with more than 50% lesioned left-hemisphere nodes also yielded significant F tests for the prediction of each WAB measure; there were some differences in significant predictors compared with the models with all of the participants, but the overall patterns are very similar (e.g., LD and RDV as frequent negative significant predictors, L&RD as a frequent positive significant predictor; Table A1).

DISCUSSION

The purpose of this study was twofold: (1) characterize the dual-stream model's network characteristics in a neurotypical control group and (2) determine the feasibility of using these dual-stream network characteristics to predict speech and language impairments in stroke survivors. Our findings indicated that: (1) the regions within the dual-stream model of speech processing do perform as an intrinsic network in resting-state fMRI; (2) stroke survivors exhibited significantly less functional connectivity of the hub regions identified by the graph theory measures compared with the neurotypical control group; and (3) functional connectivities of hub regions are significant predictors of poststroke language performance.

Dual-stream Model Represents an Intrinsic Resting-state Network

In previous studies, the intrinsic connectivity of a network is defined as an ongoing neural and metabolic activity that occurs in the resting basal state (Raichle, 2015; Kilpatrick et al., 2011; Napadow et al., 2010). After the default mode network was discovered in the resting-state (Raichle et al., 2001), many other functional networks were studied with resting-state fMRI, including but not limited to executive, salience, dorsal attention, and visual networks (Tessitore et al., 2017; Zhu et al., 2016; Napadow et al., 2010). To test if the regions identified by the dual-stream model of speech processing also can be treated as an intrinsic functional network at rest, we computed two sets of comparisons: (1) the functional connectivity within the dual-stream network compared with functional connectivity within two well-known networks—the default mode network and the visual network, and (2) the functional connectivity between each of the three main components of the dual-stream model (i.e., LD, LV, and RV) compared with between the dual-stream, default-mode, and visual networks. Our results indicated no significant difference between the strength of the functional connectivity within the default mode and within the dual-stream network, but the visual network exhibited significantly higher functional connectivity than the default mode and dual-stream network (Figure 3). It is not surprising that the visual network had the strongest functional connectivity because the locations of the visual nodes are spatially very close to one another compared with the other two networks. Although null results should be interpreted cautiously, the nonsignificant results between the default mode and dual-stream networks indicate that the strength of connections within the dual-stream network are similar to those of the default mode network. This finding suggests the intensity of the intrinsic activity within the dual-stream regions is similar to the most well-known resting-state network, which provides robust evidence for the existence of an intrinsic language network as outlined by the dual-stream model of speech processing. In addition, the connections between each of the streams were significantly stronger than the connections between the streams and the visual and default-mode networks. If the dorsal and ventral streams do not belong to the same intrinsic network, these between-stream connections would be the same or even weaker than the functional connectivity between the dual-stream regions and regions in these other networks. Based on these findings, we highly recommend that the dual-stream model can be interpreted as an intrinsic network in neurotypical adults, providing further evidence that there is potential to use resting-state functional connectivity measures of the dual-stream network to study the integrity of language circuitry in stroke survivors (Battistella et al., 2020). Our resting-state functional connectivity findings are highly consistent with previous task-based fMRI studies that have shown that regions in the dual-stream model are co-activated during a variety of language tasks (Saur et al., 2008, 2010; Hickok & Poeppel, 2004).

To further characterize the dual-stream network, we identified hub regions of the resting-state dual-stream network using graph theoretical parameters. The hub regions identified in the current study were in superior temporal and inferior frontal (pars triangularis) cortices for the dorsal stream, in the middle temporal gyrus and superior temporal gyrus for the left ventral stream, and in the superior

temporal gyrus and middle temporal gyrus for the RV stream. These regions are all implicated in numerous lesion-symptom mapping and neuroimaging studies of speech processing (Mesulam et al., 2014; Margulies & Petrides, 2013; Price, 2012; Dronkers, 2011; Vigneau et al., 2006). The left pars triangularis, that is, the anterior portion of Broca's area, is reliably implicated in speech production, including naming and phonological awareness (Kibby, Kroese, Krebbs, Hill, & Hynd, 2009; Foundas, Eure, Luevano, & Weinberger, 1998; Foundas, Leonard, Gilmore, Fennell, & Heilman, 1996). The other hub node in the dorsal stream in posterior superior temporal cortex is near areas known to be involved in sensorimotor and audiovisual integration (Rogalsky et al., 2015; Heim, Eickhoff, & Amunts, 2008). The ventral stream hubs include bilateral nodes in the mid and posterior middle temporal gyrus, overlapping with bilateral middle temporal regions that are reliably implicated in speech comprehension, particularly lexical-semantic processing (Acheson & Hagoort, 2013; Wallentin et al., 2011). Lesion-symptom mapping studies of stroke consistently identify damage in our left hemisphere middle temporal hubs as associated with auditory comprehension deficits (Rogalsky et al., 2022; Pillay, Binder, Humphries, Gross, & Book, 2017; Hickok & Poeppel, 2007; Dronkers, Wilkins, Van Valin, Redfern, & Jaeger, 2004; Bates et al., 2003). Thus, the hub nodes identified by our graph theory approach are not surprising, but it is noteworthy that the RV hubs are in the middle temporal gyrus and not the superior temporal gyrus. Most task-based neuroimaging and neurostimulation studies of speech identify more superior temporal than middle temporal regions in the right hemisphere, which is often attributed to spectrotemporal acoustic processing that is not specific to speech (Wolmetz, Poeppel, & Rapp, 2011; Hickok & Poeppel, 2007). Our findings suggest that multiple regions of the right middle temporal gyrus are highly connected with other nodes of the dual-stream network and require further study as to their role in speech processing and aphasia recovery.

Functional Connectivity Patterns in Stroke Survivors

Numerous previous studies indicate that structural damage to dual-stream cortical regions or the WM connecting them is related to various speech and language impairments in poststroke aphasia (Matchin et al., 2022; Baboyan et al., 2021; Yang et al., 2017; Agosta et al., 2013; Kümmerer et al., 2013). We see our study using functional connectivity as complementary to these structural network findings, as our graph theory analysis identified critical regions in the network, without the restraints of direct physical WM tract connectivity. Previous voxel-based lesion symptom mapping studies have identified several left ventral stream regions to be critical for auditory speech comprehension, including posterior superior temporal and middle temporal gyrus regions (Na, Jung, Tench, Auer, & Pyun, 2022; Rogalsky et al., 2022; Sul et al., 2019; Gajardo-Vidal et al., 2018; Dronkers et al., 2004; Bates et al., 2003). Speech production deficits have been associated with damage to the dorsal stream, including inferior frontal, insular, premotor, and inferior parietal regions (Na et al., 2022; Sul et al., 2019; Bates et al., 2003). Performance on tasks that involve both dorsal and ventral stream functions, such as naming or repetition, have implicated numerous dorsal and ventral regions (Na et al., 2022; Døli, Andersen Helland, Helland, & Specht, 2021; Sul et al., 2019; Baldo et al., 2013; Rogalsky, Rong, Saberi, & Hickok, 2011). Our current study corroborates these findings from voxel-based lesion symptom mapping research and further pinpoints potentially crucial nodes within these extensive brain areas. For example, pars triangularis and posterior superior temporal regions are the hubs for the dorsal stream, which implies that they are particularly critical for speech production. In addition, our functional analyses are not only limited to areas of lesion; we also can examine the potential compensation within the right hemisphere and between hemispheres. For instance, functional connectivity of the right (but not the left) ventral's hubs is a significant predictor for repetition and naming. In addition, the RDV hub connectivity is a significant predictor of overall aphasia severity, whereas LD-ventral hub connectivity is not a significant predictor of any of our aphasia measures.

We found no significant differences between the groups when examining the functional connectivity of all nodes in each stream. However, the hub nodes' functional connectivity comparisons did find significantly weaker connectivity among the hub regions of the LD stream (pars triangularis and posterior superior temporal), as well as among the hub regions of the bilateral ventral stream (left middle superior temporal gurus and posterior middle temporal gyrus, as well as right superior temporal sulcus and middle temporal gyrus), in the stroke group compared with the control group. Based on these group-level comparisons, we conclude that graph theory approaches provide meaningful information regarding network-level dysfunction poststroke and that these dual-stream hubs defined by the graph theory should be investigated further for possible sites of neurostimulation to promote language rehabilitation in stroke survivors. The majority of our stroke group has a diagnosis of aphasia (n = 25 of 28). Thus, it is likely that weakened hub node functional connectivity, rather than overall node connectivity in the dual-stream network, is strongly related to an aphasia diagnosis post left-hemisphere stroke, although future studies are needed to explore this further.

Dual-stream Functional Connectivity as a Predictor of Language Abilities

Because of the significantly lower average functional connectivity between the hub nodes in the stroke group compared with the control group, we tested the ability of these

hub functional connectivities to predict performance on subtests of the WAB, after accounting for variance because of lesion size, age, sex, and education years (Table 8).

In the ventral stream, hubs were identified bilaterally in posterior middle temporal and mid superior temporal regions. Notably, neither the functional connectivity of the hub nodes within the left ventral stream nor the functional connectivity of the left ventral hub nodes with other streams' hubs were significant predictors of performance on any WAB subtest. Perhaps partial damage to the left ventral stream does not yield a deficit on clinical measures because of the RV stream's contributions, providing additional evidence of the bilateral nature of the ventral stream. We did expect that a major damage to the left ventral nodes would yield comprehension impairments (Bonilha et al., 2017; Robson et al., 2014), but our stroke group contained only 3.5% of individuals with Wernicke's aphasia, which is often associated with large left temporal lesions. Thus, left ventral effects perhaps did not reach significance at the group level because of this small sampling of Wernicke's aphasia.

It also is noteworthy that our regression models did not find functional connectivity between the LD and ventral streams to be a significant predictor of performance on any WAB subtest, including repetition and naming, which both have been previously shown to reliably engage both left frontal and left posterior temporal cortices (Trimmel et al., 2018; Cappa, Sandrini, Rossini, Sosta, & Miniussi, 2002). However, it should be noted that for Spontaneous Speech scores, LD-ventral connectivity approaches significance ($p = .052$). To our knowledge, there is no clear theoretical basis or finding in previous work that could explain these null results, but we will speculate here, in hopes that it may be potentially helpful to direct future work. According to the dual-stream model, the dorsal stream and ventral stream communicate mainly via the auditory-motor interface in the posterior superior temporal gyrus (i.e., area Spt) and the arcuate fasciculus, as well as via WM connections between the anterior temporal lobe and inferior frontal gyrus. These connections in the dual-stream model are supported by numerous structural connectivity studies (Glasser & Rilling, 2008; Rilling et al., 2008; Saur et al., 2008). However notably, our hub nodes identified by our graph theory approach did not include any regions in the anterior temporal lobes. Thus, some of the typical communications between the two streams may not be reflected in our functional connectivity measures between the dorsal and ventral hubs. Another possibility is that the functional connectivity between the LD and ventral hub nodes may not be necessary for successful language abilities, and perhaps even the synchronization of these hub nodes may suggest network dysfunction that leads to lower performance on some language measures.

Our findings related to the right-hemisphere homologue of the LD stream (i.e., the "right dorsal" stream) may provide some clarity as to why previous work investigating potential benefits of the right hemisphere in poststroke recovery have been equivocal (François et al., 2019; Xing et al., 2016). Notably, across all WAB subtests, greater RDV functional connectivity predicted poorer performance. This finding coincides with previous evidence implying that the activity in the right hemisphere following a left-hemisphere stroke is not helpful to language rehabilitation (Richter, Miltner, & Straube, 2008; Karbe et al., 1998), that is, seemingly supporting a negative view of the compensation activity in the right hemisphere. However, our results provide a more nuanced view of the right hemisphere's contributions to poststroke speech and language abilities: While greater RDV functional connectivity was related to poorer performance and more severe aphasia, greater functional connectivity L&RD streams were significant predictors of more mild aphasia symptoms overall (i.e., a higher WAB aphasia quotient). These findings suggest that right dorsal stream contributions to poststroke speech could possibly be beneficial, but not by replacing the functionality of the LD stream, but rather supporting the remaining LD stream via more domain-general cognitive resources that have been previously located to right lateral frontal cortex (Huang et al., 2022; Reuter et al., 2011). Right frontal regions have been shown to be activated by a variety of speech and language tasks, particularly as task demands increase (van Ettinger-Veenstra et al., 2010; Just, Carpenter, Keller, Eddy, & Thulborn, 1996). It may be that the right hemisphere's dorsal stream is able to contribute to some aspects of speech-processing for which these cognitive processes may be particularly helpful, such as word selection or sentence building, but unable to support others, such as speech motor planning and control. These motor speech deficits (i.e., elements of dysarthria and apraxia of speech) are common in individuals with aphasia and contribute to performance on the WAB's expressive subtests. Future studies with more sensitive measures of motor speech deficits are needed to test this possibility.

One possible explanation to consider for the right dorsal findings is lesion size—perhaps larger left-hemisphere lesions lead to both greater speech impairments and also greater right hemisphere involvement in speech tasks, which could be reflected in greater RDV connectivity. However, this is not the case in our study: We found lesion size to be a significant predictor of performance on only one WAB subtest, Spontaneous Speech. Thus, future studies are needed to investigate the possibility of how to promote functional connectivity between left and right dorsal hubs, but not between right dorsal and ventral hubs, in individuals with aphasia to maximize this potential compensatory strategy.

Previous task-based fMRI studies have found that greater right-hemisphere activations predict greater aphasia severity (LaCroix, James, & Rogalsky, 2021; Postman-Caucheteux et al., 2010; Richter et al., 2008). Conversely, in the present study, we found that stronger RV functional connectivity was a significant predictor of better naming and repetition performance—two functions known to

engage the ventral stream in neurotypical control participants (Ross, McCoy, Wolk, Coslett, & Olson, 2010; Saur et al., 2008; Hickok & Poeppel, 2004; Wise et al., 2001). These findings provide further evidence for the bilaterality of the ventral stream of the language network. However, it is also notable that performance on the Auditory Verbal Comprehension subtest and overall aphasia severity (as measured by WAB-R Aphasia Quotient) were not predicted by RV connectivity. These differences in the predictive ability of RV connectivity across the WAB subtests may be because of the nature of the WAB's Comprehension subtest, which includes many stimuli of increasing complexity at the phrasal and sentence levels. The RV stream has been found to support single-word comprehension and phonological encoding (Hickok & Poeppel, 2007; Gorno-Tempini et al., 2004), but are not modulated by sentence structure or morphosyntactic manipulations (Novén, Schremm, Horne, & Roll, 2021; Humphries et al., 2006). Although the RV connectivity did not predict overall aphasia severity, our findings related to naming and repetition suggest that RV connectivity may help support some lexical-semantic and phonological functions in poststroke aphasia. Future studies of the RV stream's connectivity in relation to other more specific receptive speech measures are needed to characterize how the RV stream is contributing to receptive and productive speech abilities in individuals with aphasia.

Lastly, we would like to discuss our consistent finding of LD stream functional connectivity being a significant negative predictor of WAB subtest performance. On the surface, this finding was surprising: How could less coherence within the LD stream predict better performance on speech tasks known to be supported by these LD regions (e.g., spontaneous speech and repetition)? Upon further inspection of the data, it is apparent that individuals with aphasia with large left frontal lesions encompassing the LD stream hub nodes are driving this negative correlation between LD hub connectivity and WAB performance. The functional connectivity of these individuals' injured LD nodes (i.e., nodes that overlap with the lesion area) are very high compared with the functional connectivity from the intact nodes, because of the lack of fluctuation in the BOLD response of these "lesioned" nodes. In other words, the functional connectivity of their LD nodes is very strongly correlated because all of these nodes exhibit very little to no BOLD response. To our knowledge, this paradox has not been addressed in the previous literature of functional connectivity after a stroke, and thus previous characterizations of functional connectivity changes may need to be interpreted with this issue in mind (Liu et al., 2017; Zhu et al., 2014). Perhaps novel approaches need to be developed to determine how to best consider both correlation and amplitude of BOLD fluctuations to maximize the utility of using functional connectivity predictors to better understand the neurobiology of poststroke speech and language impairments.

Limitations, Alternative Approaches, and Future Directions

Our study has a few important limitations to consider. First, the effects of interscanner and intersite differences are of ongoing debate in the field (Badhwar et al., 2020; Noble et al., 2017), and our stroke and control groups' data were collected on two different scanners. The difference in number of channels in the head coil or head coil type may also bring some variability. However, in the current study, only the between-group comparisons may be affected by possible interscanner effects; the hub nodes were defined only within the control group, and the functional connectivity predictors of speech-processing abilities were only within the stroke group. Future studies can use a single-scanner data set and also consider other alternative normalization procedures for the stroke MRI data, such as using a cohort-specific template, to determine the optimal procedures for these between-group comparisons (Pappas et al., 2021).

Another methodological item that requires further consideration is how to best treat functional ROIs that include areas of structural damage (i.e., within the binary structural lesion map). Klingbeil and colleagues (2019) suggest that areas of lesion do not provide a "meaningful BOLD signal" and thus should be excluded from analyses (Klingbeil et al., 2019). Yet, previous studies (e.g., Shahid et al., 2017; Siegel et al., 2016) and visual inspection of our own data indicate that blood flow within areas delineated as having structural damage is often nonzero, and the neural activity within lesion penumbra has been associated with greater functional recovery in both chronic and acute stroke (Kroll, Zaharchuk, Christen, Heit, & Iv, 2017; Tsai et al., 2014; Zhang, Ke, Li, Yip, & Tong, 2013). Some studies have explored the impact of lesioned areas on functional connectivity analyses (Griffis, Metcalf, Corbetta, & Shulman, 2019; Saenger et al., 2018). However, there is no gold standard for how to treat lesions in functional ROIs, and numerous exclusion criteria can be found in the resting-state fMRI literature, ranging from none (e.g., Wang et al., 2021; Zhang, Xia, et al., 2021; Riccardi, Yourganov, Rorden, Fridriksson, & Desai, 2020; Balaev, Orlov, Petrushevsky, & Martynova, 2018), to preset thresholds of amount of damage (e.g., Griffis et al., 2019; Siegel et al., 2016), to exclusion of any lesioned ROIs (e.g., Klingbeil et al., 2019). Given that a focus of the present study's analyses within the stroke group was to determine if resting-state functional connectivity of the dual-stream speech network can be used to predict poststroke speech processing impairments, our primary analyses within the stroke group did not take into account areas of structural lesion; we wanted to avoid having to make assumptions about the integrity of blood flow or the quality of the BOLD signal within the lesion, or attempt to delineate areas of infarct versus penumbra. Nonetheless, we wanted to ensure that performance of stroke participants with large areas of damage encompassing most of

our dual-stream nodes were not driving results. To this end, overall lesion size was included as a predictor in our regression models. We also computed the stroke group analyses after excluding stroke participants with severe damage to the LD and ventral streams (defined as >50% of nodes damaged). The results (Figures A1, A2; Table A1) after excluding the four participants meeting this criteria remain very similar to our primary results. Our findings suggest that large lesions encompassing a majority of our functional nodes are not driving our results, although certainly future work is needed to identify optimal approaches to integrating lesion maps and functional connectivity for predicting aphasia measures.

We computed *t* tests between the stroke and control groups to identify group differences in the functional connectivities of the dual-stream speech network (all nodes, and then for hub nodes only). An alternative method to examine group differences is network-based statistics (NBS: Zalesky, Fornito, & Bullmore, 2010; https://www.nitrc.org/projects/nbs/). NBS provides more power than mass univariate testing by controlling FWE rate across all tests that are performed for each connection in the connectivity graph. NBS was not the focus of our analyses because we aimed to compare across groups the overall and hub node connectivities within the different subportions of the dual-stream network. However for comparison purposes, an exploratory post hoc NBS was computed for the entire dual-stream network. The NBS results (Figure A3) generally coincide with our original between-group comparisons of our hub nodes, with LD (precentral gyrus and pars triangularis) and left ventral (middle temporal gyrus) nodes exhibiting weaker connections in the stroke group than in the control group.

Lastly, alternative approaches to our graph theory methods to define hub nodes should also be considered. For example, normalized participation coefficients (NPCs; Pedersen, Omidvarnia, Shine, Jackson, & Zalesky, 2020) consider relative intranetwork versus internetwork connectivity, normalized by network size, to identify hub nodes. The present study focused on hubs within different portions of the dual-stream network, but considering interstream connectivity when determining hub nodes is an interesting future direction. Post hoc, for exploratory comparison purposes, we computed the NPC for each node and identified hubs as the nodes with the top two NPCs in each stream (Table A2). There is some overlap between the hubs defined by NPC versus our original average shortest path length method, but the hubs are not identical. For example, the NPC nodes in the left ventral stream are more anterior in the superior temporal lobe than our original nodes, and portions of the inferior frontal gyrus (pars opercularis) are defined as LD hubs by both methods (NPC hub in pars opercularis, original method hub in pars triangularis). Some differences are expected given that NPC considers internetwork connectivity and shortest path length does not. We also computed between-group *t* tests and regression models for these NPC-defined hubs as we did for our original hub nodes identified by the shortest path length (Table A3). Unlike for our original nodes, there were no significant differences between the stroke and control groups' functional connectivity for these NPC-defined hubs. However, like our original regression models, the NPC-defined hub models did yield significant results for predicting each aphasia measure, albeit with some different significant predictors for some of the aphasia measures.

Conclusion

In conclusion, our study has five main findings: (1) The dual-stream model is representative of an intrinsic network as measured by resting-state fMRI; (2) the functional connectivity of the hub nodes of the dual-stream network, but not overall network connectivity, is significantly lower in our stroke group than in the control group; (3) the intrinsic connectivity of the dorsal and ventral stream hubs identified in neurotypical control participants significantly predict performance on clinical aphasia measures (e.g., WAB subtests) in individuals with poststroke left hemisphere damage; (4) greater connectivity of the right dorsal with the LD stream, and less connectivity with the RV stream, significantly predicts better performance in expressive and receptive speech tasks and lower overall aphasia severity; (5) greater functional connectivity within the RV stream significantly predicts better naming and repetition performance in individuals with poststroke left hemisphere damage.

APPENDIX

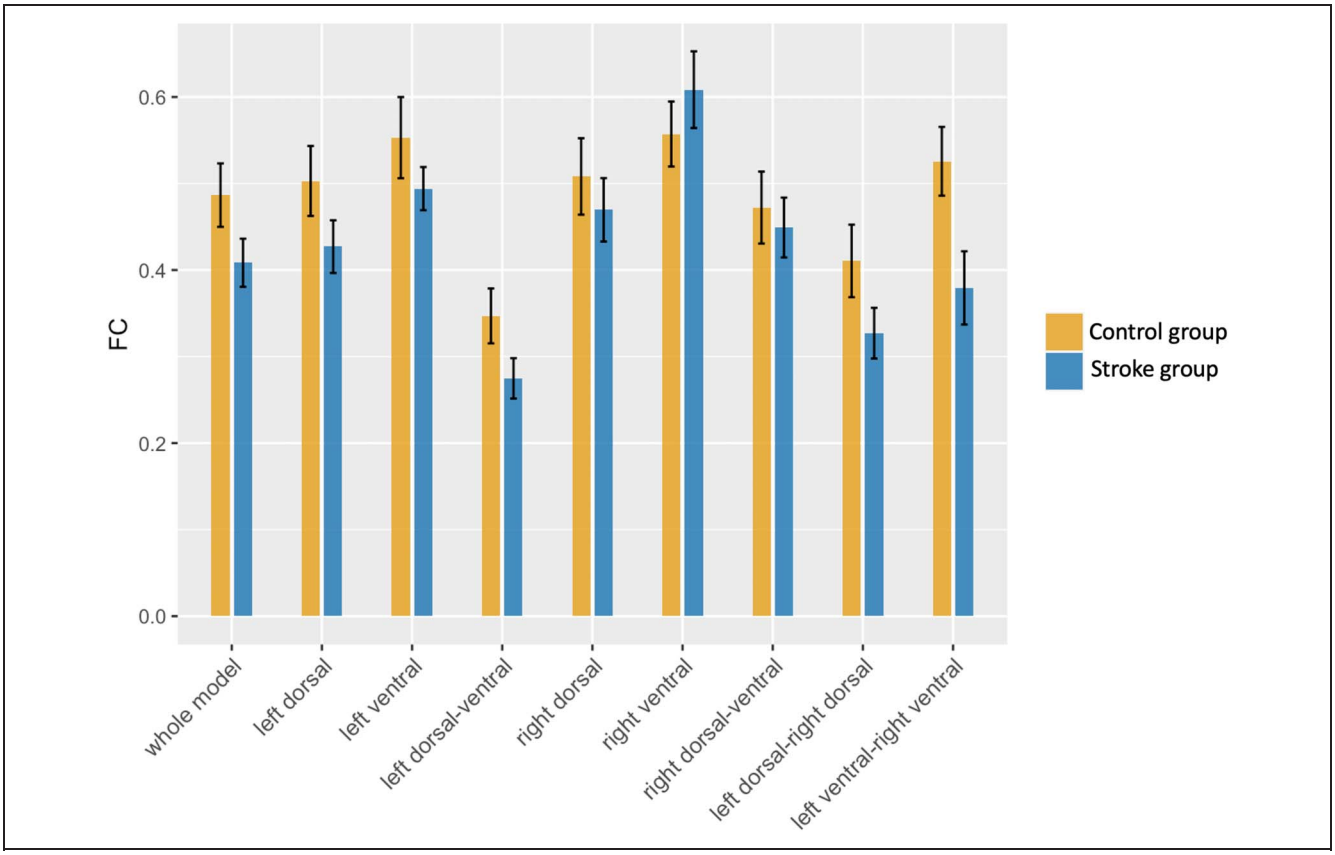

Figure A1. Between-group comparisons from the average of all nodes after excluding the four participants with more than eight lesioned nodes. *t* Tests yielded no significant differences (all *p*s > .1 after FDR correction).

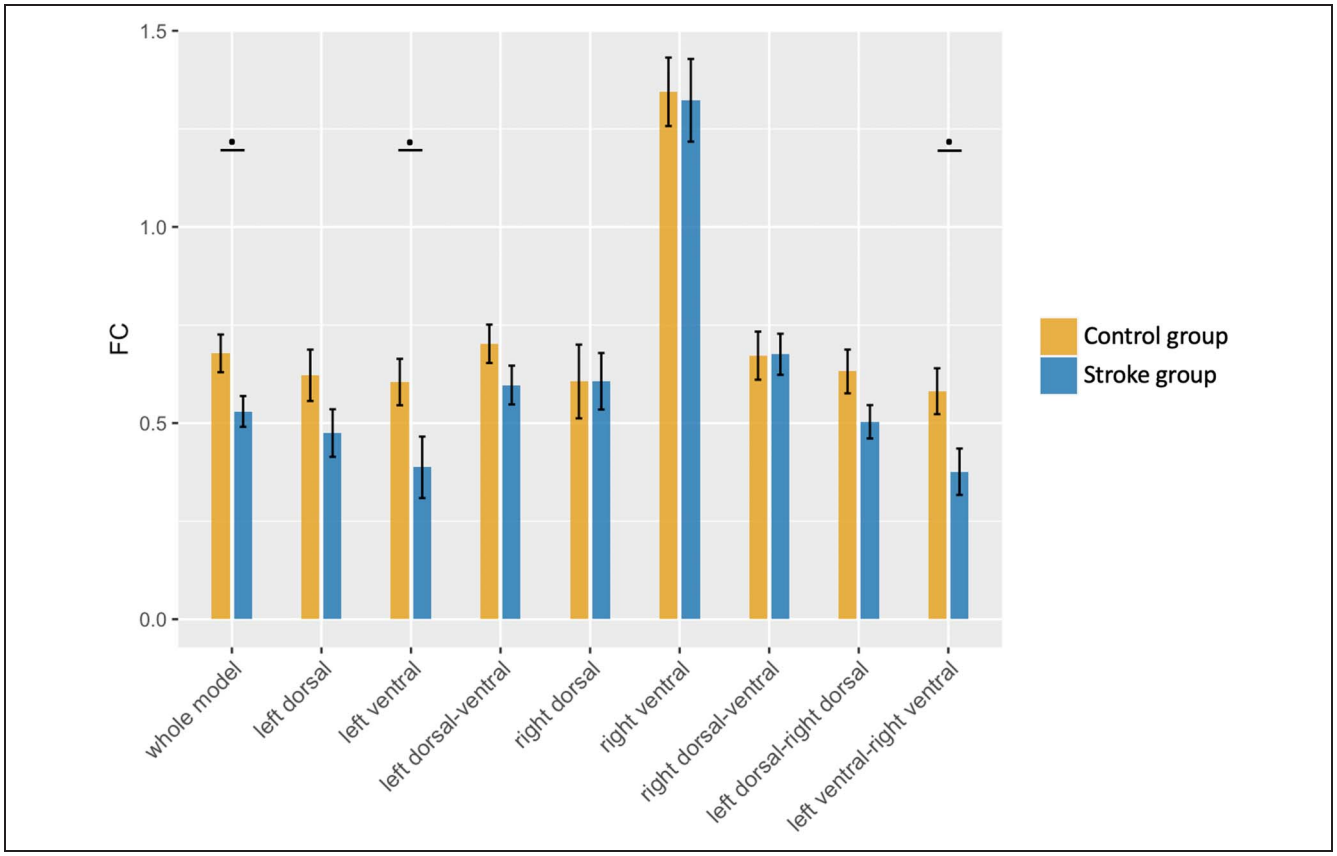

Figure A2. Between-group comparisons from hub nodes after excluding the four participants with more than eight lesioned nodes. *t* Tests yield no significant differences between groups, although three *t* tests (indicated by a dot) approach significance after FDR correction: whole model, $t(50) = 2.34$, $p = .02$, FDR $p = .087$; left ventral, $t(50) = 2.25$ $p = .03$, FDR $p = .087$; LV to RV, $t(50) = 2.45$, $p = .02$, FDR $p = .087$.

Table A1. Results of Regression Models Using the Hub Functional Connectivity Predictors after Excluding the Four Participants with More Than Eight Lesioned Nodes

	LD	*Right Dorsal*	*Left Ventral*	*RV*	*LD-Ventral*	*RDV*	*Left & Right Dorsal*	*Left & RV*	*F Test*
SS	**β = −15.83** ***t* = −3.11** ***p* = .01**	–			β = 8.45 *t* = 1.61 *p* = .13	**β = −7.83** ***t* = −2.14** ***p* = .05**	β = 9.18 *t* = 1.57 *p* = .13		***F*(7, 16) = 3.95, *p* = .01**
AVC			–	β = 1.60 *t* = 2.03 *p* = .06	–	**β = −3.83** ***t* = −2.4** ***p* = .03**		–	***F*(3, 20) = 4.53, *p* = .01**
RP	**β = −4.52** ***t* = −2.70** ***p* = .02**	β = −2.31 *t* = −1.65 *p* = .12	–	β = 1.88 *t* = 1.98 *p* = .07	–	**β = −5.11** ***t* = −2.61** ***p* = .02**	**β = 7.18** ***t* = 2.39** ***p* = .03**	–	***F*(7, 16) = 5.99, *p* < .01**
NWF	**β = −8.77** ***t* = −3.73** ***p* < .01**	–	–	**β = −3.25** ***t* = −3.73** ***p* < .01**	β = 3.72 *t* = 1.60 *p* = .13	**β = −6.56** ***t* = −3.48** ***p* < .01**	**β = 7.47** ***t* = 2.42** ***p* = .03**	β = −2.52 *t* = −1.45 *p* = .17	***F*(9, 14) = 6.24, *p* < .01**
AQ	**β = −56.12** ***t* = −2.81** ***p* = .02**	β = −19.31 *t* = −1.47 *p* = .17	–	**β = 21.30** ***t* = 2.62** ***p* = .02**	β = 21.89 *t* = 1.11 *p* = .29	**β = −41.34** ***t* = −2.38** ***p* = .03**	**β = 75.40** ***t* = 2.86** ***p* = .01**	–	***F*(10, 12) = 5.72, *p* < .01**

Significant findings are in **bold**. The first column is the dependent variable from the Western Aphasia Battery, the following columns are the functional connectivity independent variables, and the last column is the *F* test of the regression model. Dependent variables: SS = Spontaneous Speech; AVC = Auditory Verbal Comprehension; RP = Repetition; NWF = Naming and Word Finding; AQ = Aphasia Quotient. The gray color indicates the predictor is not included in the initial model. The dash indicates the predictors are removed by Akaike-Information-Criterion-based elimination.

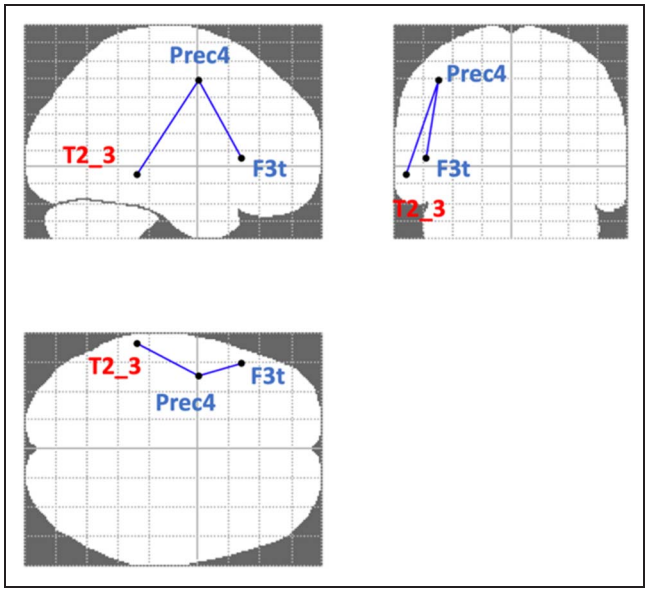

Figure A3. Post hoc exploration of alternative methods to measure between-group connectivity differences using the NBS toolbox (https://www.nitrc.org/projects/nbs/; Zalesky et al., 2010). Default or standard parameters were used to identify functional connectivity differences between the stroke and control groups using NBS (e.g., statistical test = *t* test, threshold = 3.4, permutation = 5000, significance = 0.05). This figure displays the NBS toolbox depiction of the NBS results: The functional connectivity of the stroke group is significantly lower than the control group between the left precentral gyrus (Prec4) and left pars triangularis (F3t), as well as between the left precentral gyrus and the left middle temporal gyrus (T2_3). Blue = dorsal stream node; red = ventral stream node.

Table A2. Post Hoc Exploration of an Alternative Hub Node Definition Method Using NPCs (Pedersen et al., 2020) via an In-house MATLAB Script

Category	*Region*	*Abbreviation*	*NPC*
LD	Inferior frontal pars opercularis gyrus	F3O1	0.6693
	Superior frontal gyrus	F1_2	0.6323
LV	Superior temporal sulcus – 1	STS1	0.6993
	Superior temporal sulcus – 2	STS2	0.6533
RD	*Inferior frontal pars opercularis gyrus*	*F3O1*	*0.6264*
	Superior frontal gyrus	*F1_2*	*0.7260*
RV	Superior temporal sulcus – 3	STS3	0.7454
	Superior temporal sulcus – 2	STS2	0.7221

As was done in our primary hub identification process using the shortest path length, the highest two NPCs in each stream were designated as hubs (listed here), with the exception of the right dorsal hubs (*italics*), which were identified by the homologue coordinates of the LD hubs.

Table A3. Results of the Regression Models Using NPC Hub Functional Connectivity Predictors

	LD	*Right Dorsal*	*Left Ventral*	*RV*	*LD-Ventral*	*RDV*	*Left & Right Dorsal*	*Left & RV*	*F Test*
SS	**β = −9.34** ***t* = −2.80** ***p* = .01**	–			**β = 9.98** ***t* = 3.01** ***p* < .01**	**β = −12.69** ***t* = −4.10** ***p* < .01**	**β = 10.67** ***t* = 2.41** ***p* = .03**		***F*(6, 21) = 7.24, *p* < .01**
AVC			–	β = 1.84 *t* = 1.97 *p* = .06	β = 2.31 *t* = 1.63 *p* = .11	**β = −3.98** ***t* = −3.42** ***p* < .01**		–	***F*(6, 21) = 5.55, *p* < .01**
RP	–	–	–	**β= 3.05** ***t* = 2.52** ***p* = .02**	–	**β = −7.65** ***t* = −4.27** ***p* < .01**	**β = 3.94** ***t* = 2.39** ***p* = .03**	–	***F*(6, 21) = 5.34, *p* < .01**
NWF	β = −3.97 *t* = −1.66 *p* = .11	–	–	–	β = 3.38 *t* = 1.42 *p* = .17	**β = −7.05** ***t* = −3.45** ***p* < .01**	β = 5.18 *t* = 1.73 *p* = .09	–	***F*(7, 20) = 7.27, *p* < .01**
AQ	**β = −36.41** ***t* = −2.21** ***p* = .04**	–	–	**β = 23.37** ***t* = 2.20** ***p* = .04**	β = 28.11 *t* = 1.71 *p* = .1	**β = −65.57** ***t* = −4.65** ***p* < .01**	**β = 48.84** ***t* = 2.37** ***p* = .03**	–	***F*(8, 19) = 6.39, *p* < .01**

The first column is the dependent variable from the Western Aphasia Battery, following columns are the functional connectivity independent variables, and the last column is the *F* test of the regression model. Dependent variables: SS = Spontaneous Speech; AVC = Auditory Verbal Comprehension; RP = Repetition; NWF = Naming and Word Finding; AQ = Aphasia Quotient. The significant predictors are in **bold** font. The gray color indicates the predictor is not included in the initial model. The dash indicates the predictors are removed by Akaike-Information-Criterion-based elimination.

Corresponding author: Corianne Rogalsky, Speech and Hearing Science, Arizona State University, P.O. Box 870102, Tempe, AZ 85287-0102, e-mail: corianne.rogalsky@asu.edu.

Data Availability Statement

Materials, data, and analysis scripts are available via an email request to the corresponding author.

Author Contributions

Haoze Zhu: Conceptualization; Formal analysis; Methodology; Software; Visualization; Writing—Original draft; Writing—Review & editing. Megan C. Fitzhugh: Data curation; Investigation; Writing—Review & editing. Lynsey M. Keator: Data curation; Investigation; Writing—Review & editing. Lisa Johnson: Data curation; Investigation; Writing—Review & editing. Chris Rorden: Data curation; Funding acquisition; Writing—Review & editing. Leonardo Bonilha: Data curation; Investigation; Writing—Review & editing. Julius Fridriksson: Data curation; Funding acquisition; Supervision; Writing—Review & editing. Corianne Rogalsky: Conceptualization; Funding acquisition; Supervision; Writing—Original draft; Writing—Review & editing.

Funding Information

This work is supported by Arizona State University and National Institute on Deafness and Other Communication Disorders (https://dx.doi.org/10.13039/100000055), grant number: P50 DC014664 to J. F.

Diversity in Citation Practices

Retrospective analysis of the citations in every article published in this journal from 2010 to 2021 reveals a persistent pattern of gender imbalance: Although the proportions of authorship teams (categorized by estimated gender identification of first author/last author) publishing in the *Journal of Cognitive Neuroscience* (*JoCN*) during this period were M(an)/M = .407, W(oman)/M = .32, M/W = .115, and W/W = .159, the comparable proportions for the articles that these authorship teams cited were M/M = .549, W/M = .257, M/W = .109, and W/W = .085 (Postle and Fulvio, *JoCN*, 34:1, pp. 1–3). Consequently, *JoCN* encourages all authors to consider gender balance explicitly when selecting which articles to cite and gives them the opportunity to report their article's gender citation balance.

Note

1. Speech processing is the term as shorthand for auditory speech comprehension, speech repetition, and speech production (including naming).

REFERENCES

Achard, S., & Bullmore, E. (2007). Efficiency and cost of economical brain functional networks. *PLoS Computational Biology*, *3*, e17. https://doi.org/10.1371/journal.pcbi.0030017, PubMed: 17274684

Achard, S., Salvador, R., Whitcher, B., Suckling, J., & Bullmore, E. (2006). A resilient, low-frequency, small-world human brain functional network with highly connected association cortical hubs. *Journal of Neuroscience*, *26*, 63–72. https://doi.org/10.1523/JNEUROSCI.3874-05.2006, PubMed: 16399673

Acheson, D. J., & Hagoort, P. (2013). Stimulating the brain's language network: Syntactic ambiguity resolution after TMS to the inferior frontal gyrus and middle temporal gyrus. *Journal of Cognitive Neuroscience*, *25*, 1664–1677. https://doi.org/10.1162/jocn_a_00430, PubMed: 23767923

Agosta, F., Galantucci, S., Canu, E., Cappa, S. F., Magnani, G., Franceschi, M., et al. (2013). Disruption of structural connectivity along the dorsal and ventral language pathways in patients with nonfluent and semantic variant primary progressive aphasia: A DT MRI study and a literature review. *Brain and Language*, *127*, 157–166. https://doi.org/10.1016/j.bandl.2013.06.003, PubMed: 23890877

Albert, R., Jeong, H., & Barabási, A.-L. (2000). Error and attack tolerance of complex networks. *Nature*, *406*, 378–382. https://doi.org/10.1038/35019019, PubMed: 10935628

Andersen, S. M., Rapcsak, S. Z., & Beeson, P. M. (2010). Cost function masking during normalization of brains with focal lesions: Still a necessity? *Neuroimage*, *53*, 78–84. https://doi.org/10.1016/j.neuroimage.2010.06.003, PubMed: 20542122

Ashburner, J. (2007). A fast diffeomorphic image registration algorithm. *Neuroimage*, *38*, 95–113. https://doi.org/10.1016/j.neuroimage.2007.07.007, PubMed: 17761438

Avants, B. B. (2018). Relating high-dimensional structural networks to resting functional connectivity with sparse canonical correlation analysis for neuroimaging. In *Brain morphometry* (pp. 89–104). https://doi.org/10.1007/978-1-4939-7647-8_6

Baboyan, V., Basilakos, A., Yourganov, G., Rorden, C., Bonilha, L., Fridriksson, J., et al. (2021). Isolating the white matter circuitry of the dorsal language stream: Connectome-symptom mapping in stroke induced aphasia. *Human Brain Mapping*, *42*, 5689–5702. https://doi.org/10.1002/hbm.25647, PubMed: 34469044

Badhwar, A., Collin-Verreault, Y., Orban, P., Urchs, S., Chouinard, I., Vogel, J., et al. (2020). Multivariate consistency of resting-state fMRI connectivity maps acquired on a single individual over 2.5 years, 13 sites and 3 vendors. *Neuroimage*, *205*, 116210. https://doi.org/10.1016/j.neuroimage.2019.116210, PubMed: 31593793

Balaev, V., Orlov, I., Petrushevsky, A., & Martynova, O. (2018). Functional connectivity between salience, default mode and frontoparietal networks in post-stroke depression. *Journal of Affective Disorders*, *227*, 554–562. https://doi.org/10.1016/j.jad.2017.11.044, PubMed: 29169125

Baldo, J. V., Arévalo, A., Patterson, J. P., & Dronkers, N. F. (2013). Grey and white matter correlates of picture naming: Evidence from a voxel-based lesion analysis of the Boston Naming Test. *Cortex*, *49*, 658–667. https://doi.org/10.1016/j.cortex.2012.03.001, PubMed: 22482693

Barabási, A.-L. (2012). The network takeover. *Nature Physics*, *8*, 14–16. https://doi.org/10.1038/nphys2188

Bassett, D. S., & Bullmore, E. (2006). Small-world brain networks. *Neuroscientist*, *12*, 512–523. https://doi.org/10.1177/1073858406293182, PubMed: 17079517

Bates, E., Wilson, S. M., Saygin, A. P., Dick, F., Sereno, M. I., Knight, R. T., et al. (2003). Voxel-based lesion–symptom mapping. *Nature Neuroscience*, *6*, 448–450. https://doi.org/10.1038/nn1050, PubMed: 12704393

Battistella, G., Borghesani, V., Henry, M., Shwe, W., Lauricella, M., Miller, Z., et al. (2020). Task-free functional language networks: Reproducibility and clinical application. *Journal of Neuroscience*, *40*, 1311–1320. https://doi.org/10.1523/JNEUROSCI.1485-19.2019, PubMed: 31852732

Belleau, E. L., Ehret, L. E., Hanson, J. L., Brasel, K. J., Larson, C. L., & deRoon-Cassini, T. A. (2020). Amygdala functional connectivity in the acute aftermath of trauma prospectively predicts severity of posttraumatic stress symptoms. *Neurobiology of Stress*, *12*, 100217. https://doi.org/10.1016/j.ynstr.2020.100217, PubMed: 32435666

Binder, J. R., Frost, J. A., Hammeke, T. A., Bellgowan, P., Rao, S. M., & Cox, R. W. (1999). Conceptual processing during the conscious resting state: A functional MRI study. *Journal of Cognitive Neuroscience*, *11*, 80–93. https://doi.org/10.1162/089892999563265, PubMed: 9950716

Boccaletti, S., Latora, V., Moreno, Y., Chavez, M., & Hwang, D.-U. (2006). Complex networks: Structure and dynamics. *Physics Reports*, *424*, 175–308. https://doi.org/10.1016/j.physrep.2005.10.009

Bohland, J., Kapse, K., & Kiran, S. (2014). Graph analytic characterization of resting state networks in post-stroke aphasia. In *Academy of aphasia—52nd Annual Meeting*, Miami, FL. https://doi.org/10.3389/conf.fpsyg.2014.64.00050

Bonilha, L., Hillis, A. E., Hickok, G., Den Ouden, D. B., Rorden, C., & Fridriksson, J. (2017). Temporal lobe networks supporting the comprehension of spoken words. *Brain*, *140*, 2370–2380. https://doi.org/10.1093/brain/awx169, PubMed: 29050387

Braun, U., Plichta, M. M., Esslinger, C., Sauer, C., Haddad, L., Grimm, O., et al. (2012). Test–retest reliability of resting-state connectivity network characteristics using fMRI and graph theoretical measures. *Neuroimage*, *59*, 1404–1412. https://doi.org/10.1016/j.neuroimage.2011.08.044, PubMed: 21888983

Brett, M., Leff, A. P., Rorden, C., & Ashburner, J. (2001). Spatial normalization of brain images with focal lesions using cost function masking. *Neuroimage*, *14*, 486–500. https://doi.org/10.1006/nimg.2001.0845, PubMed: 11467921

Cappa, S. F., Sandrini, M., Rossini, P. M., Sosta, K., & Miniussi, C. (2002). The role of the left frontal lobe in action naming: rTMS evidence. *Neurology*, *59*, 720–723. https://doi.org/10.1212/wnl.59.5.720, PubMed: 12221163

Carter, A. R., Shulman, G. L., & Corbetta, M. (2012). Why use a connectivity-based approach to study stroke and recovery of function? *Neuroimage*, *62*, 2271–2280. https://doi.org/10.1016/j.neuroimage.2012.02.070, PubMed: 22414990

Chambers, J. M., & Hastie, T. J. (Eds.) (1992). *Statistical models in S.* Pacific Grove, CA: Wadsworth & Brooks/Cole.

Chen, X., Chen, L., Zheng, S., Wang, H., Dai, Y., Chen, Z., et al. (2021). Disrupted brain connectivity networks in aphasia revealed by resting-state fMRI. *Frontiers in Aging Neuroscience*, *13*, 666301. https://doi.org/10.3389/fnagi.2021.666301, PubMed: 34744682

Cordes, D., Haughton, V. M., Arfanakis, K., Wendt, G. J., Turski, P. A., Moritz, C. H., et al. (2000). Mapping functionally related regions of brain with functional connectivity MR imaging. *American Journal of Neuroradiology*, *21*, 1636–1644. PubMed: 11039342

Crinion, J., & Price, C. J. (2005). Right anterior superior temporal activation predicts auditory sentence comprehension following aphasic stroke. *Brain*, *128*, 2858–2871. https://doi.org/10.1093/brain/awh659, PubMed: 16234297

Døli, H., Andersen Helland, W., Helland, T., & Specht, K. (2021). Associations between lesion size, lesion location and aphasia in acute stroke. *Aphasiology*, *35*, 745–763. https://doi.org/10.1080/02687038.2020.1727838

Dormann, C. F., Elith, J., Bacher, S., Buchmann, C., Carl, G., Carré, G., et al. (2013). Collinearity: A review of methods to deal with it and a simulation study evaluating their performance. *Ecography*, *36*, 27–46. https://doi.org/10.1111/j.1600-0587.2012.07348.x

Dronkers, N. F. (2011). The neural architecture of the language comprehension network: Converging evidence from lesion and connectivity analyses. *Frontiers in Systems Neuroscience*, *5*, 1. https://doi.org/10.3389/fnsys.2011.00001, PubMed: 21347218

Dronkers, N. F., Wilkins, D. P., Van Valin, R. D., Jr., Redfern, B. B., & Jaeger, J. J. (2004). Lesion analysis of the brain areas involved in language comprehension. *Cognition*, *92*, 145–177. https://doi.org/10.1016/j.cognition.2003.11.002, PubMed: 15037129

Duncan, E. S., & Small, S. L. (2016). Increased modularity of resting state networks supports improved narrative production in aphasia recovery. *Brain Connectivity*, *6*, 524–529. https://doi.org/10.1089/brain.2016.0437, PubMed: 27345466

Ferguson, M. A., Lim, C., Cooke, D., Darby, R. R., Wu, O., Rost, N. S., et al. (2019). A human memory circuit derived from brain lesions causing amnesia. *Nature Communications*, *10*, 1–9. https://doi.org/10.1038/s41467-019-11353-z, PubMed: 31375668

Fitzhugh, M. C., Hemesath, A., Schaefer, S. Y., Baxter, L. C., & Rogalsky, C. (2019). Functional connectivity of Heschl's gyrus associated with age-related hearing loss: A resting-state fMRI study. *Frontiers in Psychology*, *10*, 2485. https://doi.org/10.3389/fpsyg.2019.02485, PubMed: 31780994

Fitzhugh, M. C., Schaefer, S. Y., Baxter, L. C., & Rogalsky, C. (2021). Cognitive and neural predictors of speech comprehension in noisy backgrounds in older adults. *Language, Cognition and Neuroscience*, *36*, 269–287. https://doi.org/10.1080/23273798.2020.1828946, PubMed: 34250179

Foundas, A. L., Eure, K. F., Luevano, L. F., & Weinberger, D. R. (1998). MRI asymmetries of Broca's area: The pars triangularis and pars opercularis. *Brain and Language*, *64*, 282–296. https://doi.org/10.1006/brln.1998.1974, PubMed: 9743543

Foundas, A. L., Leonard, C. M., Gilmore, R. L., Fennell, E. B., & Heilman, K. M. (1996). Pars triangularis asymmetry and language dominance. *Proceedings of the National Academy of Sciences, U.S.A.*, *93*, 719–722. https://doi.org/10.1073/pnas.93.2.719, PubMed: 8570622

François, C., Ripollés, P., Ferreri, L., Muchart, J., Sierpowska, J., Fons, C., et al. (2019). Right structural and functional reorganization in four-year-old children with perinatal arterial ischemic stroke predict language production. *Eneuro*, *6*. https://doi.org/10.1523/ENEURO.0447-18.2019, PubMed: 31383726

Fridriksson, J., den Ouden, D.-B., Hillis, A. E., Hickok, G., Rorden, C., Basilakos, A., et al. (2018). Anatomy of aphasia revisited. *Brain*, *141*, 848–862. https://doi.org/10.1093/brain/awx363, PubMed: 29360947

Gajardo-Vidal, A., Lorca-Puls, D. L., Crinion, J. T., White, J., Seghier, M. L., Leff, A. P., et al. (2018). How distributed processing produces false negatives in voxel-based lesion-deficit analyses. *Neuropsychologia*, *115*, 124–133. https://doi.org/10.1016/j.neuropsychologia.2018.02.025, PubMed: 29477839

Gao, W., & Lin, W. (2012). Frontal parietal control network regulates the anti-correlated default and dorsal attention networks. *Human Brain Mapping*, *33*, 192–202. https://doi.org/10.1002/hbm.21204, PubMed: 21391263

Glasser, M. F., & Rilling, J. K. (2008). DTI tractography of the human brain's language pathways. *Cerebral Cortex*, *18*, 2471–2482. https://doi.org/10.1093/cercor/bhn011, PubMed: 18281301

Griffis, J. C., Metcalf, N. V., Corbetta, M., & Shulman, G. L. (2019). Structural disconnections explain brain network dysfunction after stroke. *Cell Reports*, *28*, 2527–2540. https://doi.org/10.1016/j.celrep.2019.07.100, PubMed: 31484066

Gorno-Tempini, M. L., Dronkers, N. F., Rankin, K. P., Ogar, J. M., Phengrasamy, L., Rosen, H. J., et al. (2004). Cognition and anatomy in three variants of primary progressive aphasia.

Annals of Neurology, *55*, 335–346. https://doi.org/10.1002/ana.10825, PubMed: 14991811
Hampson, M., Peterson, B. S., Skudlarski, P., Gatenby, J. C., & Gore, J. C. (2002). Detection of functional connectivity using temporal correlations in MR images. *Human Brain Mapping*, *15*, 247–262. https://doi.org/10.1002/hbm.10022, PubMed: 11835612
He, Y., Chen, Z., & Evans, A. (2008). Structural insights into aberrant topological patterns of large-scale cortical networks in Alzheimer's disease. *Journal of Neuroscience*, *28*, 4756–4766. https://doi.org/10.1523/JNEUROSCI.0141-08.2008, PubMed: 18448652
He, Y., & Evans, A. (2010). Graph theoretical modeling of brain connectivity. *Current Opinion in Neurology*, *23*, 341–350. https://doi.org/10.1097/WCO.0b013e32833aa567, PubMed: 20581686
Heim, S., Eickhoff, S. B., & Amunts, K. (2008). Specialisation in Broca's region for semantic, phonological, and syntactic fluency? *Neuroimage*, *40*, 1362–1368. https://doi.org/10.1016/j.neuroimage.2008.01.009, PubMed: 18296070
Hickok, G., & Poeppel, D. (2000). Towards a functional neuroanatomy of speech perception. *Trends in Cognitive Sciences*, *4*, 131–138. https://doi.org/10.1016/s1364-6613(00)01463-7, PubMed: 10740277
Hickok, G., & Poeppel, D. (2004). Dorsal and ventral streams: A framework for understanding aspects of the functional anatomy of language. *Cognition*, *92*, 67–99. https://doi.org/10.1016/j.cognition.2003.10.011, PubMed: 15037127
Hickok, G., & Poeppel, D. (2007). The cortical organization of speech processing. *Nature Reviews Neuroscience*, *8*, 393–402. https://doi.org/10.1038/nrn2113, PubMed: 17431404
Huang, W., Li, X., Xie, H., Qiao, T., Zheng, Y., Su, L., et al. (2022). Different cortex activation and functional connectivity in executive function between young and elder people during Stroop Test: An fNIRS study. *Frontiers in Aging Neuroscience*, *14*, 864662. https://doi.org/10.3389/fnagi.2022.864662, PubMed: 35992592
Humphries, M. D., Gurney, K., & Prescott, T. J. (2006). The brainstem reticular formation is a small-world, not scale-free, network. *Proceedings of the Royal Society of London, Series B: Biological Sciences*, *273*, 503–511. https://doi.org/10.1098/rspb.2005.3354, PubMed: 16615219
Humphries, C., Willard, K., Buchsbaum, B., & Hickok, G. (2001). Role of anterior temporal cortex in auditory sentence comprehension: An fMRI study. *NeuroReport*, *12*, 1749–1752. https://doi.org/10.1097/00001756-200106130-00046, PubMed: 11409752
Just, M. A., Carpenter, P. A., Keller, T. A., Eddy, W. F., & Thulborn, K. R. (1996). Brain activation modulated by sentence comprehension. *Science*, *274*, 114–116. https://doi.org/10.1126/science.274.5284.114, PubMed: 8810246
Karbe, H., Thiel, A., Weber-Luxenburger, G., Herholz, K., Kessler, J., & Heiss, W.-D. (1998). Brain plasticity in poststroke aphasia: What is the contribution of the right hemisphere? *Brain and Language*, *64*, 215–230. https://doi.org/10.1006/brln.1998.1961, PubMed: 9710490
Keator, L. M., Yourganov, G., Basilakos, A., Hillis, A. E., Hickok, G., Bonilha, L., et al. (2021). Independent contributions of structural and functional connectivity: Evidence from a stroke model. *Network Neuroscience*, *5*, 911–928. https://doi.org/10.1162/netn_a_00207, PubMed: 35024536
Keator, L. M., Yourganov, G., Faria, A. V., Hillis, A. E., & Tippett, D. C. (2022). Application of the dual stream model to neurodegenerative disease: Evidence from a multivariate classification tool in primary progressive aphasia. *Aphasiology*, *36*, 618–647. https://doi.org/10.1080/02687038.2021.1897079, PubMed: 35493273
Kertesz, A. (2007). *Western aphasia battery–Revised*. https://doi.org/10.1037/t15168-000
Kertesz, A. (2022). The Western Aphasia Battery: A systematic review of research and clinical applications. *Aphasiology*, *36*, 21–50. https://doi.org/10.1080/02687038.2020.1852002
Khazaee, A., Ebrahimzadeh, A., & Babajani-Feremi, A. (2015). Identifying patients with Alzheimer's disease using resting-state fMRI and graph theory. *Clinical Neurophysiology*, *126*, 2132–2141. https://doi.org/10.1016/j.clinph.2015.02.060, PubMed: 25907414
Kibby, M. Y., Kroese, J. M., Krebbs, H., Hill, C. E., & Hynd, G. W. (2009). The pars triangularis in dyslexia and ADHD: A comprehensive approach. *Brain and Language*, *111*, 46–54. https://doi.org/10.1016/j.bandl.2009.03.001, PubMed: 19356794
Kilpatrick, L. A., Suyenobu, B. Y., Smith, S. R., Bueller, J. A., Goodman, T., Creswell, J. D., et al. (2011). Impact of mindfulness-based stress reduction training on intrinsic brain connectivity. *Neuroimage*, *56*, 290–298. https://doi.org/10.1016/j.neuroimage.2011.02.034, PubMed: 21334442
Klingbeil, J., Wawrzyniak, M., Stockert, A., & Saur, D. (2019). Resting-state functional connectivity: An emerging method for the study of language networks in post-stroke aphasia. *Brain and Cognition*, *131*, 22–33. https://doi.org/10.1016/j.bandc.2017.08.005, PubMed: 28865994
Kroll, H., Zaharchuk, G., Christen, T., Heit, J. J., & Iv, M. (2017). Resting-state BOLD MRI for perfusion and ischemia. *Topics in Magnetic Resonance Imaging*, *26*, 91–96. https://doi.org/10.1097/RMR.0000000000000119, PubMed: 28277456
Kümmerer, D., Hartwigsen, G., Kellmeyer, P., Glauche, V., Mader, I., Klöppel, S., et al. (2013). Damage to ventral and dorsal language pathways in acute aphasia. *Brain*, *136*, 619–629. https://doi.org/10.1093/brain/aws354, PubMed: 23378217
Labache, L., Joliot, M., Saracco, J., Jobard, G., Hesling, I., Zago, L., et al. (2019). A SENtence Supramodal areas AtlaS (SENSAAS) based on multiple task-induced activation mapping and graph analysis of intrinsic connectivity in 144 healthy right-handers. *Brain Structure and Function*, *224*, 859–882. https://doi.org/10.1007/s00429-018-1810-2, PubMed: 30535758
LaCroix, A. N., James, E., & Rogalsky, C. (2021). Neural resources supporting language production vs. comprehension in chronic post-stroke aphasia: A meta-analysis using activation likelihood estimates. *Frontiers in Human Neuroscience*, *15*, 680933. https://doi.org/10.3389/fnhum.2021.680933, PubMed: 34759804
Lee, M. H., Smyser, C. D., & Shimony, J. S. (2013). Resting-state fMRI: A review of methods and clinical applications. *American Journal of Neuroradiology*, *34*, 1866–1872. https://doi.org/10.3174/ajnr.A3263, PubMed: 22936095
Liao, X., Vasilakos, A. V., & He, Y. (2017). Small-world human brain networks: Perspectives and challenges. *Neuroscience & Biobehavioral Reviews*, *77*, 286–300. https://doi.org/10.1016/j.neubiorev.2017.03.018, PubMed: 28389343
Liu, Y., Liang, M., Zhou, Y., He, Y., Hao, Y., Song, M., et al. (2008). Disrupted small-world networks in schizophrenia. *Brain*, *131*, 945–961. https://doi.org/10.1093/brain/awn018, PubMed: 18299296
Liu, J., Wang, Q., Liu, F., Song, H., Liang, X., Lin, Z., et al. (2017). Altered functional connectivity in patients with post-stroke memory impairment: A resting fMRI study. *Experimental and Therapeutic Medicine*, *14*, 1919–1928. https://doi.org/10.3892/etm.2017.4751, PubMed: 28962104
Marek, S., Tervo-Clemmens, B., Nielsen, A. N., Wheelock, M. D., Miller, R. L., Laumann, T. O., et al. (2019). Identifying reproducible individual differences in childhood functional brain networks: An ABCD study. *Developmental Cognitive*

Neuroscience, *40*, 100706. https://doi.org/10.1016/j.dcn.2019.100706, PubMed: 31614255
Margulies, D. S., & Petrides, M. (2013). Distinct parietal and temporal connectivity profiles of ventrolateral frontal areas involved in language production. *Journal of Neuroscience*, *33*, 16846–16852. https://doi.org/10.1523/JNEUROSCI.2259-13.2013, PubMed: 24133284
Maslov, S., & Sneppen, K. (2002). Specificity and stability in topology of protein networks. *Science*, *296*, 910–913. https://doi.org/10.1126/science.1065103, PubMed: 11988575
Matchin, W., den Ouden, D.-B., Hickok, G., Hillis, A. E., Bonilha, L., & Fridriksson, J. (2022). The Wernicke conundrum revisited: Evidence from connectome-based lesion-symptom mapping. *Brain*, *145*, 3916–3930. https://doi.org/10.1093/brain/awac219, PubMed: 35727949
Mazrooyisebdani, M., Nair, V. A., Garcia-Ramos, C., & Prabhakaran, V. (2018). Abstract TP145: Evolution of language network plasticity post stroke based on graph theory. *Stroke*, *49(Suppl. 1)*, ATP145. https://doi.org/10.1161/str.49.suppl_1.TP145
Mesulam, M.-M., Rogalski, E. J., Wieneke, C., Hurley, R. S., Geula, C., Bigio, E. H., et al. (2014). Primary progressive aphasia and the evolving neurology of the language network. *Nature Reviews Neurology*, *10*, 554–569. https://doi.org/10.1038/nrneurol.2014.159, PubMed: 25179257
Montoya, J. M., & Solé, R. V. (2002). Small world patterns in food webs. *Journal of Theoretical Biology*, *214*, 405–412. https://doi.org/10.1006/jtbi.2001.2460, PubMed: 11846598
Muller, A. M., & Meyer, M. (2014). Language in the brain at rest: New insights from resting state data and graph theoretical analysis. *Frontiers in Human Neuroscience*, *8*, 228. https://doi.org/10.3389/fnhum.2014.00228, PubMed: 24808843
Na, Y., Jung, J., Tench, C. R., Auer, D. P., & Pyun, S. B. (2022). Language systems from lesion-symptom mapping in aphasia: A meta-analysis of voxel-based lesion mapping studies. *Neuroimage: Clinical*, *35*, 103038. https://doi.org/10.1016/j.nicl.2022.103038, PubMed: 35569227
Napadow, V., LaCount, L., Park, K., As-Sanie, S., Clauw, D. J., & Harris, R. E. (2010). Intrinsic brain connectivity in fibromyalgia is associated with chronic pain intensity. *Arthritis & Rheumatism*, *62*, 2545–2555. https://doi.org/10.1002/art.27497, PubMed: 20506181
Noble, S., Scheinost, D., Finn, E. S., Shen, X., Papademetris, X., McEwen, S. C., et al. (2017). Multisite reliability of MR-based functional connectivity. *Neuroimage*, *146*, 959–970. https://doi.org/10.1016/j.neuroimage.2016.10.020, PubMed: 27746386
Novén, M., Schremm, A., Horne, M., & Roll, M. (2021). Cortical thickness and surface area of left anterior temporal areas affects processing of phonological cues to morphosyntax. *Brain Research*, *1750*, 147150. https://doi.org/10.1016/j.brainres.2020.147150, PubMed: 33039411
Pappas, I., Hector, H., Haws, K., Curran, B., Kayser, A. S., & D'Esposito, M. (2021). Improved normalization of lesioned brains via cohort-specific templates. *Human Brain Mapping*, *42*, 4187–4204. https://doi.org/10.1002/hbm.25474, PubMed: 34143540
Pedersen, M., Omidvarnia, A., Shine, J. M., Jackson, G. D., & Zalesky, A. (2020). Reducing the influence of intramodular connectivity in participation coefficient. *Network Neuroscience*, *4*, 416–431. https://doi.org/10.1162/netn_a_00127, PubMed: 32537534
Pillay, S. B., Binder, J. R., Humphries, C., Gross, W. L., & Book, D. S. (2017). Lesion localization of speech comprehension deficits in chronic aphasia. *Neurology*, *88*, 970–975. https://doi.org/10.1212/WNL.0000000000003683, PubMed: 28179469
Postman-Caucheteux, W. A., Birn, R. M., Pursley, R. H., Butman, J. A., Solomon, J. M., Picchioni, D., et al. (2010). Single-trial fMRI shows contralesional activity linked to overt naming errors in chronic aphasic patients. *Journal of Cognitive Neuroscience*, *22*, 1299–1318. https://doi.org/10.1162/jocn.2009.21261, PubMed: 19413476
Price, C. J. (2012). A review and synthesis of the first 20 years of PET and fMRI studies of heard speech, spoken language and reading. *Neuroimage*, *62*, 816–847. https://doi.org/10.1016/j.neuroimage.2012.04.062, PubMed: 22584224
Raichle, M. E. (2015). The brain's default mode network. *Annual Review of Neuroscience*, *38*, 433–447. https://doi.org/10.1146/annurev-neuro-071013-014030, PubMed: 25938726
Raichle, M. E., MacLeod, A. M., Snyder, A. Z., Powers, W. J., Gusnard, D. A., & Shulman, G. L. (2001). A default mode of brain function. *Proceedings of the National Academy of Sciences, U.S.A.*, *98*, 676–682. https://doi.org/10.1073/pnas.98.2.676, PubMed: 11209064
Reuter, F., Zaaraoui, W., Crespy, L., Faivre, A., Rico, A., Malikova, I., et al. (2011). Cognitive impairment at the onset of multiple sclerosis: Relationship to lesion location. *Multiple Sclerosis Journal*, *17*, 755–758. https://doi.org/10.1177/1352458511398265, PubMed: 21372116
Riccardi, N., Yourganov, G., Rorden, C., Fridriksson, J., & Desai, R. (2020). Degradation of praxis brain networks and impaired comprehension of manipulable nouns in stroke. *Journal of Cognitive Neuroscience*, *32*, 467–483. https://doi.org/10.1162/jocn_a_01495, PubMed: 31682566
Richter, M., Miltner, W. H., & Straube, T. (2008). Association between therapy outcome and right-hemispheric activation in chronic aphasia. *Brain*, *131*, 1391–1401. https://doi.org/10.1093/brain/awn043, PubMed: 18349055
Rilling, J. K., Glasser, M. F., Preuss, T. M., Ma, X., Zhao, T., Hu, X., et al. (2008). The evolution of the arcuate fasciculus revealed with comparative DTI. *Nature Neuroscience*, *11*, 426–428. https://doi.org/10.1038/nn2072, PubMed: 18344993
Robson, H., Zahn, R., Keidel, J. L., Binney, R. J., Sage, K., & Lambon Ralph, M. A. (2014). The anterior temporal lobes support residual comprehension in Wernicke's aphasia. *Brain*, *137*, 931–943. https://doi.org/10.1093/brain/awt373, PubMed: 24519979
Rogalsky, C., Basilakos, A., Rorden, C., Pillay, S., LaCroix, A. N., Keator, L., et al. (2022). The neuroanatomy of speech processing: A large-scale lesion study. *Journal of Cognitive Neuroscience*, *34*, 1355–1375. https://doi.org/10.1162/jocn_a_01876, PubMed: 35640102
Rogalsky, C., & Hickok, G. (2009). Selective attention to semantic and syntactic features modulates sentence processing networks in anterior temporal cortex. *Cerebral Cortex*, *19*, 786–796. https://doi.org/10.1093/cercor/bhn126, PubMed: 18669589
Rogalsky, C., Poppa, T., Chen, K.-H., Anderson, S. W., Damasio, H., Love, T., et al. (2015). Speech repetition as a window on the neurobiology of auditory–motor integration for speech: A voxel-based lesion symptom mapping study. *Neuropsychologia*, *71*, 18–27. https://doi.org/10.1016/j.neuropsychologia.2015.03.012, PubMed: 25777496
Rogalsky, C., Rong, F., Saberi, K., & Hickok, G. (2011). Functional anatomy of language and music perception: Temporal and structural factors investigated using functional magnetic resonance imaging. *Journal of Neuroscience*, *31*, 3843–3852. https://doi.org/10.1523/JNEUROSCI.4515-10.2011, PubMed: 21389239
Roger, E., Pichat, C., Torlay, L., David, O., Renard, F., Banjac, S., et al. (2019). Hubs disruption in mesial temporal lobe epilepsy. A resting-state fMRI study on a language-and-memory

network. *Human Brain Mapping*, *41*, 779–796. https://doi.org/10.1002/hbm.24839, PubMed: 31721361
Ross, L. A., McCoy, D., Wolk, D. A., Coslett, H. B., & Olson, I. R. (2010). Improved proper name recall by electrical stimulation of the anterior temporal lobes. *Neuropsychologia*, *48*, 3671–3674. https://doi.org/10.1016/j.neuropsychologia.2010.07.024, PubMed: 20659489
Saenger, V. M., Ponce-Alvarez, A., Adhikari, M., Hagmann, P., Deco, G., & Corbetta, M. (2018). Linking entropy at rest with the underlying structural connectivity in the healthy and lesioned brain. *Cerebral Cortex*, *28*, 2948–2958. https://doi.org/10.1093/cercor/bhx176, PubMed: 28981635
Saur, D., Kreher, B. W., Schnell, S., Kümmerer, D., Kellmeyer, P., Vry, M.-S., et al. (2008). Ventral and dorsal pathways for language. *Proceedings of the National Academy of Sciences, U.S.A.*, *105*, 18035–18040. https://doi.org/10.1073/pnas.0805234105, PubMed: 19004769
Saur, D., Schelter, B., Schnell, S., Kratochvil, D., Küpper, H., Kellmeyer, P., et al. (2010). Combining functional and anatomical connectivity reveals brain networks for auditory language comprehension. *Neuroimage*, *49*, 3187–3197. https://doi.org/10.1016/j.neuroimage.2009.11.009, PubMed: 19913624
Schöpf, V., Kasess, C., Lanzenberger, R., Fischmeister, F., Windischberger, C., & Moser, E. (2010). Fully exploratory network ICA (FENICA) on resting-state fMRI data. *Journal of Neuroscience Methods*, *192*, 207–213. https://doi.org/10.1016/j.jneumeth.2010.07.028, PubMed: 20688104
Shahid, H., Sebastian, R., Schnur, T. T., Hanayik, T., Wright, A., Tippett, D. C., et al. (2017). Important considerations in lesion-symptom mapping: Illustrations from studies of word comprehension. *Human Brain Mapping*, *38*, 2990–3000. https://doi.org/10.1002/hbm.23567, PubMed: 28317276
Shrestha, N. (2020). Detecting multicollinearity in regression analysis. *American Journal of Applied Mathematics and Statistics*, *8*, 39–42. https://doi.org/10.12691/ajams-8-2-1
Shulman, G. L., Fiez, J. A., Corbetta, M., Buckner, R. L., Miezin, F. M., Raichle, M. E., et al. (1997). Common blood flow changes across visual tasks: II. Decreases in cerebral cortex. *Journal of Cognitive Neuroscience*, *9*, 648–663. https://doi.org/10.1162/jocn.1997.9.5.648, PubMed: 23965122
Siegel, J. S., Ramsey, L. E., Snyder, A. Z., Metcalf, N. V., Chacko, R. V., Weinberger, K., et al. (2016). Disruptions of network connectivity predict impairment in multiple behavioral domains after stroke. *Proceedings of the National Academy of Sciences, U.S.A.*, *113*, E4367–E4376. https://doi.org/10.1073/pnas.1521083113, PubMed: 27402738
Spitsyna, G., Warren, J. E., Scott, S. K., Turkheimer, F. E., & Wise, R. J. (2006). Converging language streams in the human temporal lobe. *Journal of Neuroscience*, *26*, 7328–7336. https://doi.org/10.1523/JNEUROSCI.0559-06.2006, PubMed: 16837579
Stam, C., De Haan, W., Daffertshofer, A., Jones, B., Manshanden, I., van Cappellen van Walsum, A.-M., et al. (2009). Graph theoretical analysis of magnetoencephalographic functional connectivity in Alzheimer's disease. *Brain*, *132*, 213–224. https://doi.org/10.1093/brain/awn262, PubMed: 18952674
Stockbridge, M. D., Faria, A. V., Fridriksson, J., Rorden, C., Bonilha, L., & Hillis, A. E. (2023). Subacute aphasia recovery is associated with resting-state connectivity within and beyond the language network. *Annals of Clinical and Translational Neurology*, *10*, 1525–1532. https://doi.org/10.1002/acn3.51842, PubMed: 37403712
Stone, J. R., Avants, B. B., Tustison, N. J., Wassermann, E. M., Gill, J., Polejaeva, E., et al. (2020). Functional and structural neuroimaging correlates of repetitive low-level blast exposure in career breachers. *Journal of Neurotrauma*, *37*, 2468–2481. https://doi.org/10.1089/neu.2020.7141, PubMed: 32928028
Sul, B., Lee, K. B., Hong, B. Y., Kim, J. S., Kim, J., Hwang, W. S., et al. (2019). Association of lesion location with long-term recovery in post-stroke aphasia and language deficits. *Frontiers in Neurology*, *10*, 776. https://doi.org/10.3389/fneur.2019.00776, PubMed: 31396146
Tedeschi, G., Russo, A., Conte, F., Corbo, D., Caiazzo, G., Giordano, A., et al. (2016). Increased interictal visual network connectivity in patients with migraine with aura. *Cephalalgia*, *36*, 139–147. https://doi.org/10.1177/0333102415584360, PubMed: 25926619
Tessitore, A., De Micco, R., Giordano, A., di Nardo, F., Caiazzo, G., Siciliano, M., et al. (2017). Intrinsic brain connectivity predicts impulse control disorders in patients with Parkinson's disease. *Movement Disorders*, *32*, 1710–1719. https://doi.org/10.1002/mds.27139, PubMed: 28949049
Thye, M., & Mirman, D. (2018). Relative contributions of lesion location and lesion size to predictions of varied language deficits in post-stroke aphasia. *NeuroImage: Clinical*, *20*, 1129–1138. https://doi.org/10.1016/j.nicl.2018.10.017, PubMed: 30380520
Tie, Y., Rigolo, L., Norton, I. H., Huang, R. Y., Wu, W., Orringer, D., et al. (2014). Defining language networks from resting-state fMRI for surgical planning—A feasibility study. *Human Brain Mapping*, *35*, 1018–1030. https://doi.org/10.1002/hbm.22231, PubMed: 23288627
Tombaugh, T. N., & McIntyre, N. J. (1992). The Mini-Mental State Examination: A comprehensive review. *Journal of the American Geriatrics Society*, *40*, 922–935. https://doi.org/10.1111/j.1532-5415.1992.tb01992.x, PubMed: 1512391
Trimmel, K., van Graan, A. L., Caciagli, L., Haag, A., Koepp, M. J., Thompson, P. J., et al. (2018). Left temporal lobe language network connectivity in temporal lobe epilepsy. *Brain*, *141*, 2406–2418. https://doi.org/10.1093/brain/awy164, PubMed: 29939211
Tsai, Y. H., Yuan, R., Huang, Y. C., Weng, H. H., Yeh, M. Y., Lin, C. P., et al. (2014). Altered resting-state FMRI signals in acute stroke patients with ischemic penumbra. *PLoS One*, *9*, e105117. https://doi.org/10.1371/journal.pone.0105117, PubMed: 25121486
Van Den Heuvel, M. P., & Pol, H. E. H. (2010). Exploring the brain network: A review on resting-state fMRI functional connectivity. *European Neuropsychopharmacology*, *20*, 519–534. https://doi.org/10.1016/j.euroneuro.2010.03.008, PubMed: 20471808
Van Dijk, K. R., Sabuncu, M. R., & Buckner, R. L. (2012). The influence of head motion on intrinsic functional connectivity MRI. *Neuroimage*, *59*, 431–438. https://doi.org/10.1016/j.neuroimage.2011.07.044, PubMed: 21810475
van Ettinger-Veenstra, H. M., Ragnehed, M., Hällgren, M., Karlsson, T., Landtblom, A.-M., Lundberg, P., et al. (2010). Right-hemispheric brain activation correlates to language performance. *Neuroimage*, *49*, 3481–3488. https://doi.org/10.1016/j.neuroimage.2009.10.041, PubMed: 19853040
Vandenberghe, R., Nobre, A. C., & Price, C. J. (2002). The response of left temporal cortex to sentences. *Journal of Cognitive Neuroscience*, *14*, 550–560. https://doi.org/10.1162/08989290260045800, PubMed: 12126497
Vigneau, M., Beaucousin, V., Hervé, P.-Y., Duffau, H., Crivello, F., Houde, O., et al. (2006). Meta-analyzing left hemisphere language areas: Phonology, semantics, and sentence processing. *Neuroimage*, *30*, 1414–1432. https://doi.org/10.1016/j.neuroimage.2005.11.002, PubMed: 16413796
Vincent, J. L., Kahn, I., Snyder, A. Z., Raichle, M. E., & Buckner, R. L. (2008). Evidence for a frontoparietal control system revealed by intrinsic functional connectivity. *Journal of Neurophysiology*, *100*, 3328–3342. https://doi.org/10.1152/jn.90355.2008, PubMed: 18799601

Wallentin, M., Nielsen, A. H., Vuust, P., Dohn, A., Roepstorff, A., & Lund, T. E. (2011). BOLD response to motion verbs in left posterior middle temporal gyrus during story comprehension. *Brain and Language*, *119*, 221–225. https://doi.org/10.1016/j.bandl.2011.04.006, PubMed: 21612817

Walsh, M. J., Baxter, L. C., Smith, C. J., & Braden, B. B. (2019). Age group differences in executive network functional connectivity and relationships with social behavior in men with autism spectrum disorder. *Research in Autism Spectrum Disorders*, *63*, 63–77. https://doi.org/10.1016/j.rasd.2019.02.008, PubMed: 32405319

Wang, S., Rao, B., Chen, L., Chen, Z., Fang, P., Miao, G., & Liao, W. (2021). Using fractional amplitude of low-frequency fluctuations and functional connectivity in patients with post-stroke cognitive impairment for a simulated stimulation program. *Frontiers in Aging Neuroscience*, *13*, 724267. https://doi.org/10.3389/fnagi.2021.724267, PubMed: 34483891

Watts, D. J., & Strogatz, S. H. (1998). Collective dynamics of 'small-world' networks. *Nature*, *393*, 440–442. https://doi.org/10.1038/30918

Wise, R. J., Scott, S. K., Blank, S. C., Mummery, C. J., Murphy, K., & Warburton, E. A. (2001). Separate neural subsystems within 'Wernicke's area'. *Brain*, *124*, 83–95. https://doi.org/10.1093/brain/124.1.83, PubMed: 11133789

Wolmetz, M., Poeppel, D., & Rapp, B. (2011). What does the right hemisphere know about phoneme categories? *Journal of Cognitive Neuroscience*, *23*, 552–569. https://doi.org/10.1162/jocn.2010.21495, PubMed: 20350179

Xiao, Y., Friederici, A. D., Margulies, D. S., & Brauer, J. (2016). Longitudinal changes in resting-state fMRI from age 5 to age 6 years covary with language development. *Neuroimage*, *128*, 116–124. https://doi.org/10.1016/j.neuroimage.2015.12.008, PubMed: 26690809

Xie, X., Hu, P., Tian, Y., Qiu, B., Wang, K., & Bai, T. (2023). Abnormal resting-state function within language network and its improvement among post-stroke aphasia. *Behavioural Brain Research*, *443*, 114344. https://doi.org/10.1016/j.bbr.2023.114344, PubMed: 36781021

Xing, S., Lacey, E. H., Skipper-Kallal, L. M., Jiang, X., Harris-Love, M. L., Zeng, J., et al. (2016). Right hemisphere grey matter structure and language outcomes in chronic left hemisphere stroke. *Brain*, *139*, 227–241. https://doi.org/10.1093/brain/awv323, PubMed: 26521078

Xu, L., Huang, L., Cui, W., & Yu, Q. (2020). Reorganized functional connectivity of language centers as a possible compensatory mechanism for basal ganglia aphasia. *Brain Injury*, *34*, 430–437. https://doi.org/10.1080/02699052.2020.1716995, PubMed: 31955634

Yang, M., Li, Y., Li, J., Yao, D., Liao, W., & Chen, H. (2017). Beyond the arcuate fasciculus: Damage to ventral and dorsal language pathways in aphasia. *Brain Topography*, *30*, 249–256. https://doi.org/10.1007/s10548-016-0503-5, PubMed: 27324257

Zalesky, A., Fornito, A., & Bullmore, E. T. (2010). Network-based statistic: Identifying differences in brain networks. *Neuroimage*, *53*, 1197–1207. https://doi.org/10.1016/j.neuroimage.2010.06.041, PubMed: 20600983

Zhang, C., Xia, Y., Feng, T., Yu, K., Zhang, H., Sami, M. U., et al. (2021). Disrupted functional connectivity within and between resting-state networks in the subacute stage of post-stroke aphasia. *Frontiers in Neuroscience*, *15*, 746264. https://doi.org/10.3389/fnins.2021.746264, PubMed: 34924929

Zhang, J., Kucyi, A., Raya, J., Nielsen, A. N., Nomi, J. S., Damoiseaux, J. S., et al. (2021). What have we really learned from functional connectivity in clinical populations? *Neuroimage*, *242*, 118466. https://doi.org/10.1016/j.neuroimage.2021.118466, PubMed: 34389443

Zhang, S. J., Ke, Z., Li, L., Yip, S. P., & Tong, K. Y. (2013). EEG patterns from acute to chronic stroke phases in focal cerebral ischemic rats: Correlations with functional recovery. *Physiological Measurement*, *34*, 423–435. https://doi.org/10.1088/0967-3334/34/4/423, PubMed: 23524534

Zhao, Y., Ralph, M. A. L., & Halai, A. D. (2018). Relating resting-state hemodynamic changes to the variable language profiles in post-stroke aphasia. *Neuroimage: Clinical*, *20*, 611–619. https://doi.org/10.1016/j.nicl.2018.08.022, PubMed: 30186765

Zhu, D., Chang, J., Freeman, S., Tan, Z., Xiao, J., Gao, Y., et al. (2014). Changes of functional connectivity in the left frontoparietal network following aphasic stroke. *Frontiers in Behavioral Neuroscience*, *8*, 167. https://doi.org/10.3389/fnbeh.2014.00167, PubMed: 24860452

Zhu, H., Zhou, P., Alcauter, S., Chen, Y., Cao, H., Tian, M., et al. (2016). Changes of intranetwork and internetwork functional connectivity in Alzheimer's disease and mild cognitive impairment. *Journal of Neural Engineering*, *13*, 046008. https://doi.org/10.1088/1741-2560/13/4/046008, PubMed: 27247279